UNIVERSIDADE TECNOLÓGICA FEDERAL DO PARANÁ

OFFICE OF RESEARCH AND GRADUATE STUDIES

GRADUATE PROGRAM IN COMPUTER SCIENCE

EDUARDO EL AKKARI SALLUM

OPTIMIZATION OF RADIO RESOURCE MANAGEMENT IN LORA NETWORKS

DISSERTATION

PONTA GROSSA

2020

EDUARDO EL AKKARI SALLUM

OPTIMIZATION OF RADIO RESOURCE MANAGEMENT IN LORA NETWORKS

Dissertation presented to the Graduate Program In Computer Science of the Department of Informatics of the Universidade Tecnológica Federal do Paraná.

Advisor: Max Mauro Dias Santos
Co-Advisor: Nuno Alexandre Magalhães Pereira

PONTA GROSSA
2020

Ficha catalográfica elaborada pelo Departamento de Biblioteca
da Universidade Tecnológica Federal do Paraná, Campus Ponta Grossa
n.64/20

S169 Sallum, Eduardo El Akkari

Optimization of radio resource management in LoRa networks. / Eduardo El Akkari Sallum, 2020.
61 f. : il. ; 30 cm.

Orientador: Prof. Dr. Max Mauro Dias Santos
Coorientador: Prof. Dr. Nuno Alexandre Magalhães Pereira

Dissertação (Mestrado em Ciência da Computação) - Programa de Pós-Graduação em Ciência da Computação. Universidade Tecnológica Federal do Paraná, Ponta Grossa, 2020.

1. Internet das coisas. 2. Sistemas de comunicação sem fio. 3. Programação linear. 4. Serviços ao cliente. 5. Desempenho - Avaliação. I. Santos, Max Mauro Dias. II. Pereira, Nuno Alexandre Magalhães. III. Universidade Tecnológica Federal do Paraná. IV. Título.

CDD 004

Elson Heraldo Ribeiro Junior. CRB-9/1413. 14/09/2020.

FOLHA DE APROVAÇÃO

Título de Dissertação Nº 20 /2020

IMPROVING QUALITY-OF-SERVICE IN LORA LOW-POWER WIDE-AREA NETWORKS THROUGH OPTIMIZED RADIO RESOURCE MANAGEMENT

Por

Eduardo El Akkari Sallum

Esta dissertação foi apresentada às **14 horas** do dia **30 de junho de 2020**, em **ambiente virtual**, como requisito parcial para a obtenção do título de MESTRE EM CIÊNCIA DA COMPUTAÇÃO, Programa de Pós-Graduação em Ciência da Computação. O candidato foi arguido pela Banca Examinadora, composta pelos professores abaixo assinados. Após deliberação, a Banca Examinadora considerou o trabalho APROVADO.

Prof. Dr. Maurício Zadra Pacheco (UEPG)

Prof. Dr. Murilo Oliveira Leme (UTFPR)

Prof. Dr. Augusto Foronda (UTFPR)

Prof. Dr. Abel Guilhermino da Silva Filho (UFPE)

Prof. Dr. Max Mauro Dias Santos (UTFPR)
Orientador e presidente da banca

Universidade Tecnológica Federal do Paraná
Campus Ponta Grossa

Visto do Coordenador:

Prof. Dr. André Koscianski
Coordenador do PPGCC
UTFPR – Câmpus Ponta Grossa

I dedicate this work
to my fiancee Cecilia.

AGRADECIMENTOS

Agradeço primeiramente a Deus por ser justo e fiel.

Agradeço ao meu pai Miguel Sallum, a minha tia Marli Sallum, ao meu irmão Guilherme Sallum e aos amigos André Batista, Aleffer Rocha, Alison Chaicoski, Bauke Dijkstra, Cesar Los Dias, Everton Skeika, Fábia Enembreck, Lin Yu Han, Rafael Garcia, e Pedro Stolle por todo o suporte, momentos de alegrias e companheirismo.

Também agradeço ao meu orientador Max Mauro Dias Santos, ao meu coorientador Nuno Magalhães Pereira e ao professor Mário Alves por todo o aprendizado, apoio e paciência para a execução deste trabalho.

Por último, agradeço a minha noiva Cecilia Ricaczeski por sempre me apoiar nos momentos difíceis e sempre estar ao meu lado.

"Be the change you want to see in the world"
- Mahatma Gandhi

RESUMO

SALLUM, Eduardo El Akkari. ***Otimização de gerenciamento de recursos de rádio em redes LoRa***. *2020*. 61 p. Dissertação, Universidade Tecnológica Federal Do Paraná. Ponta Grossa, 2020.

As redes de longa distância e baixa potência (LPWAN) permitem um número crescente de aplicativos de Internet das Coisas (IoT) com grande cobertura geográfica, baixa taxa de bits e requisitos de longa vida útil. LoRa (Long Range) é uma tecnologia LPWAN que utiliza a camada física proprietária *Chirp Spread Spectrum* (CSS), enquanto as camadas superiores são definidas por um padrão aberto - LoRaWAN. Nesta dissertação, propomos um método simples, porém eficaz, para melhorar a Qualidade-de-Serviço (QoS) das redes LoRaWAN ajustando parâmetros de rádio específicos. Através da formulação de um problema *Programação Linear Inteira Mista* (MILP), encontramos as configurações ideais para os parâmetros de rádio *Spreading Factor* (SF) e *Carrier Frequency* (CF), considerando as especificações de tráfego da rede como um todo, para aumentar o Data Extraction Rate (DER), reduzir a taxa de colisão de pacotes e o Consumo de Energia de Rede LoRa. A eficácia do procedimento de otimização é demonstrada por simulações, usando o simulador *LoRaSim* para diferentes escalas de rede. Em relação às políticas tradicionais de atribuição de parâmetros de rádio LoRa, nossa solução obteve a um aumento médio de 6% no DER e uma taxa de colisões de pacotes 13 vezes menor. Em comparação com redes com políticas de atribuição dinâmica de parâmetros de rádio, há um aumento de 5%, 2,8% e 2% de DER e um número de colisões 11, 7,8 e 2,5 vezes menor que distribuição igualitária, *Tiurlikova* e aleatória, respectivamente. Em relação à métrica Consumo de Energia da Rede, a otimização proposta obteve um consumo médio semelhante ao *Tiurlikova's* e 2,8 vezes menor que as políticas de alocação dinâmica distribuição igualitária e aleatória. Além disso, abordamos os aspectos práticos de como implementar e integrar o mecanismo de otimização proposto no LoRa, garantindo retrocompatibilidade com o protocolo padrão.

Palavras-chave: Internet das Coisas (IoT). LPWAN. Programação Linear Inteira Mista (MILP). LoRaWAN. Qualidade de Serviço (QoS). Avaliação de desempenho.

ABSTRACT

SALLUM, Eduardo El Akkari. ***Optimization of radio resource management in LoRa networks***. *2020*. 61 p. Dissertation, Universidade Tecnológica Federal do Paraná. Ponta Grossa, 2020.

Low Power Wide Area Networks (LPWAN) enable a growing number of Internet-of-Things (IoT) applications with large geographical coverage, low bit-rate, and long lifetime requirements. LoRa (Long Range) is a well-known LPWAN technology that uses a proprietary *Chirp Spread Spectrum* (CSS) physical layer, while the upper layers are defined by an open standard - LoRaWAN. In this work, we propose a simple yet effective method to improve the Quality-of-Service (QoS) of LoRaWAN networks by fine-tuning specific radio parameters. Through a *Mixed Integer Linear Programming* (MILP) problem formulation, we find optimal settings for the *Spreading Factor* (SF) and *Carrier Frequency* (CF) radio parameters, considering the network traffic specifications as a whole, to improve the *Data Extraction Rate* (DER) and to reduce the *packet collision rate* and the energy consumption in LoRa networks. The effectiveness of the optimization procedure is demonstrated by simulations, using *LoRaSim* for different network scales. About the traditional LoRa radio parameter assignment policies, our solution leads to an average increase of 6% in DER, and a *number of collisions* 13 times smaller. In comparison to networks with dynamic radio parameter assignment policies, there is an increase of 5%, 2.8%, and 2% of DER, and a *number of collisions* 11, 7.8 and 2.5 times smaller than *equal-distribution*, *Tiurlikova's* (SOTA), and *random* distribution, respectively. Regarding the *network energy consumption* metric, the proposed optimization obtained an average consumption similar to *Tiurlikova's*, and 2.8 times lower than the *equal-distribution* and *random* dynamic allocation policies. Furthermore, we approach the practical aspects of how to implement and integrate the optimization mechanism proposed in LoRa, guaranteeing backward compatibility with the standard protocol.

Key-words: Internet of Things (IoT). Low-Power Wide Area Network (LPWAN). Mixed Integer Linear Programming (MILP). LoRaWAN. LoRa Simulator (LoRaSim). Quality-of-Service (QoS). Performance evaluation.

LIST OF FIGURES

LIST OF TABLES

LIST OF SYMBOLS AND ABBREVIATIONS

ADR	*Adaptive Data Rate*
BW	*Bandwidth*
CF	*Carrier Frequency*
CPU	*Central Processing Unit*
CR	*Coding Rate*
CSS	*Chirp Spread Spectrum*
DER	*Data Extraction Rate*
FEC	*Forward Error Correction*
IoT	*Internet of Things*
LoRa	*Low Range*
LoRaSim	*LoRa Simulator*
LPWAN	*Low Power Wide Area Network*
QoS	*Quality of Service*
MAC	*Medium Access Control*
MILP	*Mixed Integer Linear Programming*
PHY	*Physical Layer*
SF	*Spreading Factor*
SNR	*Signal to Noise Ratio*
TP	*Transmission Power*
UTFPR	*Universidade Tecnológica Federal do Paraná*

SUMMARY

1 INTRODUCTION

We are at the dawn of the next generation of the Internet, which will be dominated by trillions of tiny computing devices embedded in everyday objects—the paradigm usually dubbed as Internet-of-Things (IoT). Many communication technologies can be used to interconnect IoT devices, e.g., short-range communication technologies such as Bluetooth, ZigBee, and Z-Wave. However, such technologies face critical challenges in terms of energy, cost, and complexity when applications require covering large geographical areas and feature a large number of devices, due to the need for tricky multi-hop routing in potentially harsh environments. Recent standards/technologies for Low-Power Wide-Area Networks (LPWAN) are an effective way to overcome such challenges and pave the way for new IoT applications that cover wide geographical areas over long distances (ANGRISANI et al., 2017).

The research on IoT communication protocols focused on short-range communications and applications that cover wide areas still face critical challenges regarding energy, cost, and complexity. To overcome energy challenges, emerging standards for Low-Power Wide Area-Networks (LP-WAN) enable long-range communications with low energy consumption, such that resource-constrained sensors can communicate across kilometers and operate using batteries for up to 10 years without external power sources (CENTENARO et al., 2016). The LPWAN protocols supply the requirements of IoT applications that cover large areas with minimal infrastructure (BARRETO et al., 2016).

LPWAN technologies such as LoRa (Long Range) (COMMITTEE et al., 2017), SigFox (SIGFOX, 2019), Weightless (WEIGHTLESS SIG, 2019), WAVIoT (WAVIOT, 2019), and Wi-Fi HaLow (WI-FI ALLIANCE, 2019) compete for an increasing market share among other IoT technologies, with a projected market worth of 65 Billion USD and smart gas and water metering applications occupying 20% of the LPWAN market by 2025 (GLOBAL MARKET INSIGHTS, 2019). Figure 1 shows how LPWAN compares to other wireless technologies in terms of range and Bandwidth (BW).

Figure 1 – Mapping radio coverage vs. bandwidth of wireless technologies

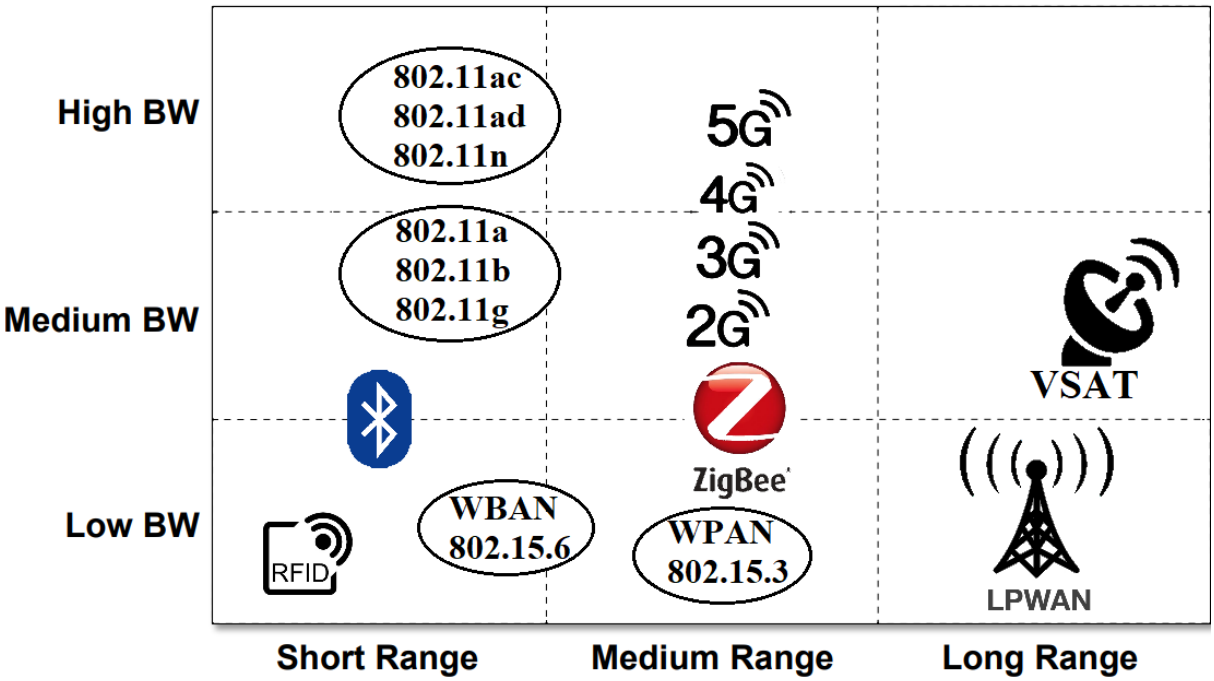

Source: Adapted from Egli (2015)

This work focuses on LoRa, a proprietary physical layer protocol that affords low-power and long-distance communication through Chirp Spread Spectrum (CSS) modulation. The main advantages of LoRa over other LPWAN technologies are the open-source MAC protocol LoRaWAN specification, low-cost application availability, and community support (COMMITTEE et al., 2017). For example, "The Things Network" is a crowd-sourced community from 85 countries building public and global IoT networks based on LoRa (THE THINGS INDUSTRIES, 2019b). Figure 2 illustrates the applications of LoRa technology in a smart city.

Figure 2 – Applications of LoRa technology in a smart city

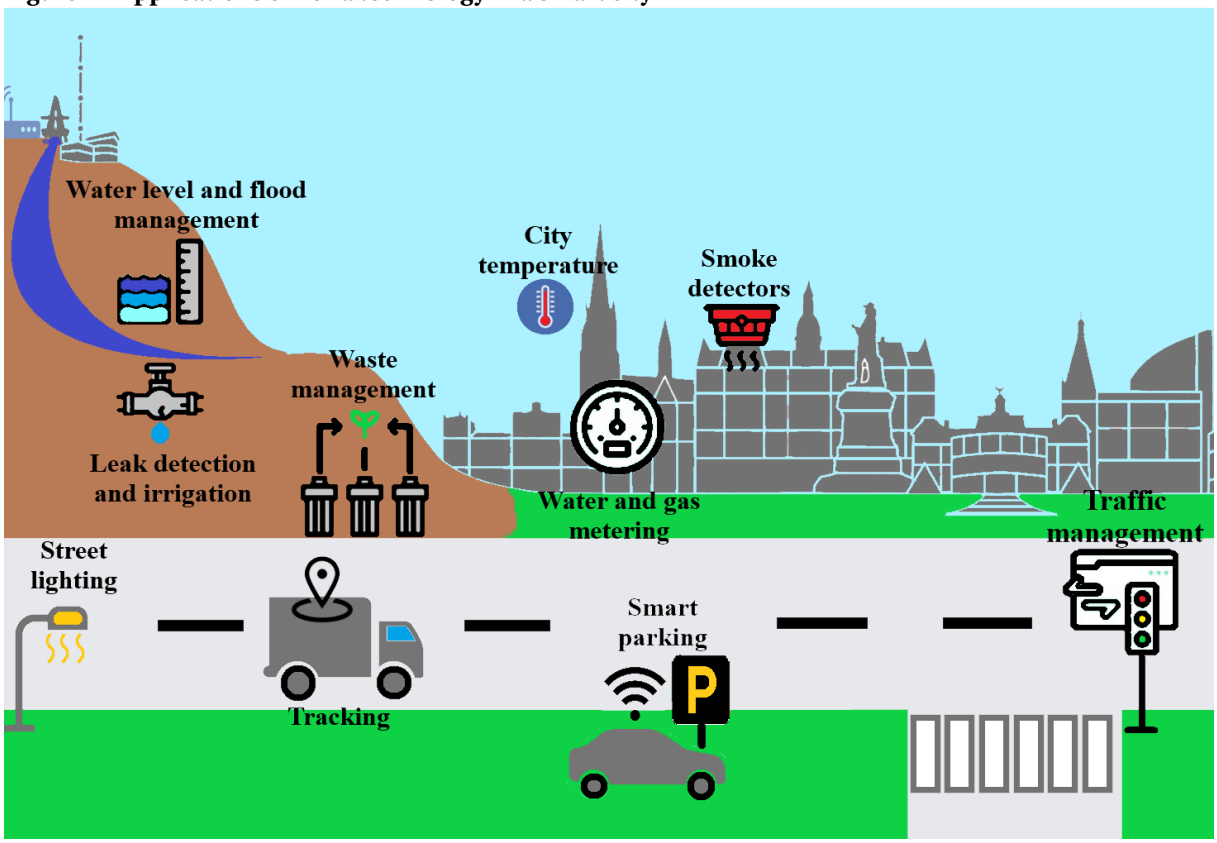

Source: Authorship.

According to Figure 2, LoRa applications include leakage and irrigation control, water level and flood management, waste management, city temperature, street lighting, GPS tracking for vehicles, smart parking, smoke detectors and smart traffic management.

The configurations of a LoRa device are set to use different propagation factors, bandwidth settings, encoding rate, and transmission power, resulting in more than 6720 possible parameter settings (BOR; ROEDIG, 2017). The physical layer LoRa implements the CSS transmission method. The characteristics of LoRa are based on the following configurable parameters:

Bandwidth (BW): BW is the width of the frequencies in the transmission band. Higher BW values provide a higher data transfer rate and greater sensitivity to noise. The sets of BW in LoRa are 125, 250, and 500 kHz.

Spreading Factor (SF): SF is the ratio between the symbol rate and the chip rate, which can be in the range of 7–12. Higher SF increases the SNR, transmission range, and packet airtime, therefore it decreases the data rate. SFs are imperfectly orthogonal. However, for traceability purposes in our experiments, they are considered orthogonal. If different SFs are used, the gateway can successfully decode multiple simultaneous data packets. LoRa modulation transmits the data at a chip rate equal to the programmed BW (chip-per-second-per-Hertz). The symbol rate and the bitrate are proportional to the BW. With CSS, each LoRa symbol is coded with a spreading code of 2^{SF} chips. Then, it takes 2^{SF} chips ($SF =$

$SFbits \times 2^{SF}$) to spread a symbol (NOREEN; BOUNCEUR; CLAVIER, 2017).

Carrier Frequency (CF): CF is the center frequency and can be programmed in a range of 137 MHz to 1020 MHz according to current geographic region legislation. For example, Table 1 shows the range of frequencies for each CF parameter, sub-bands, and max-duty-cycle (per hour) according to the ETSI EN300.220 European continent standard (THE THINGS INDUSTRIES, 2019c). In Brazil, the frequency approved by Anatel is 915 MHz (ANATEL, 2015).

Table 1 – LoRa frequencies, sub-bands, and max-duty-cycle according to CF.

CF	Frequency	Sub-Band	Max-Duty-Cycle
CF1	868.1 MHz	g1	1%
CF2	868.3 MHz	g1	1%
CF3	868.5 MHz	g1	1%
CF4	867.1 MHz	g	1%
CF5	867.3 MHz	g	1%
CF6	867.5 MHz	g	1%
CF7	867.7 MHz	g	1%
CF8	867.9 MHz	g	1%

Source: Authorship.

Transmission Power (TP): Due to hardware limitations, the TP in a LoRa network can be configured in steps of 1 dB with a signal power between 2 and 20 dBm and a service level of 1% from 17 dBm (BOR et al., 2016).

Coding Rate (CR): LoRa modulation adds Forward Error Correction (FEC), protecting against transmission interference by encoding 4-bit data with 5–8-bit redundancies, allowing the receiver to detect and correct errors in the message. The CR values are 4/5, 4/6, 4/7, and 4/8, proportional to the FEC. This means that, if the code rate is denoted as $k = N$, where k represents useful information, and the encoder generates N number of output bits, then $N - k$ will be the redundant bits. Higher CR values provide greater interference protection. However, it increases the air time. LoRa devices with different CR can switch to communicate with each other through an explicit header stored in the packet header (NAVARRO-ORTIZ et al., 2018).

1.1 MOTIVATION

According to industry experts, four out of ten long-range IoT connections are expected to be powered by LPWAN, with LoRaWAN being the dominant technology (IOT ANALYTICS, 2020). Also, Semtech® in partnership with Helium® expands LoRaWAN network deployments, offering connectivity to up to hundreds of millions of LoRa-based devices in more than 1,000 cities in North America and Europe (GLOBAL MARKET INSIGHTS, 2020). In Brazil,

the technology company Net Sensors®, specialized in the development of sustainable solutions for smart cities, launched smart culverts to fight dengue with low-cost LoRa technology (TERRA, 2020). Also, LoRa technology has helped combat Covid-19 through the development of an oximeter via LoRa connection for remote monitoring of patients by researchers from Rio de Janeiro (UFOP, 2020).

The configuration of LoRaWAN networks may be a challenging task, especially as the network scales up in the number of nodes. The link layer, LoRa, has some specific radio-related parameters that can be adjusted, such as *Carrier Frequency (CF)*, *Spreading Factor (SF)*, *Bandwidth (BW)*, *Transmission Power (TP)*, and *Coding Rate* (CR). These parameters can be tuned at a device and/or network level to enhance overall network performance, namely reducing energy consumption, improving radio coverage, and reducing radio interference and error rates. However, despite the increasing adoption of LoRa in IoT applications, the tools, methods, and models available to manage and optimize its performance are still scarce. Therefore, we propose an optimization method for selecting LoRa parameters to assist the network designer. The effectiveness of the proposed optimization procedure is demonstrated by simulations, using *LoRaSim* for different network scales, showing that our solution performs better than standard and other benchmarking radio parameter assignment policies.

1.2 GENERAL OBJECTIVES

The general objective of this work is to improve the management of radio resources in LoRa networks.

1.3 SPECIFIC OBJECTIVES

Through the formulation of a *Mixed Integer Linear Programming* problem, which generates optimal settings for the *Spreading Factor* and *Carrier Frequency* parameters, the specific objectives of this work are:

(i) Increase the *Data Extraction Rate (DER)*, which provides a network-wide measure of the valid packets received in a numerical range;

(ii) Reduce the *number of collisions*;

(iii) Reduce the network energy consumption;

Our LoRaWAN-based solution takes as input a list of available CF and SF parameters to each node, allowing for pruning settings found to be inadequate (e.g., an SF that is unusable due to distance).

1.4 CONTRIBUTIONS

The main contributions of this work are:

(i) Definition of a mathematical optimization formulation of the problem of assigning SF and CF parameters according to the traffic characteristics of LoRa end-devices;

(ii) Definition of an approximation algorithm that leads to results very close to the optimal, but with an execution time that grows much slower as the number of end-devices in the network scales;

(iii) Describe an approach to implement and integrate an algorithm for approximating the radio parameter assignment optimization method, which generates optimal results shorter execution time in LoRaWAN networks. Also analyzing, the overhead imposed by this approximation algorithm to guarantee compatibility with the standard protocol;

(iv) Implementation of the proposed optimization algorithms and other baseline policies (benchmarks to which our method is compared against in Section 4.3), and as well as of the Adaptive Data Rate (ADR) mechanism (not implemented in *LoRaSim*) in the *LoRaSim* open-source simulator, making our code available to the community (SALLUM et al., 2019); and

(v) Comparative performance analysis of six radio parameter assignment policies, showing the merit of the two proposed parameter assignment methods to the other four policies that we consider as benchmarks.

1.5 PUBLISHED PAPERS AND CONFERENCES ATTENDED

1.5.1 Published Papers

E. Sallum, N. Pereira, M. Alves, and M. Santos, "Performance optimization on LoRa networks through assigning radio parameters," In *Proc. 2020 IEEE International Conference on Industrial Technology (ICIT)*, p. 304-309, Buenos Aires, Argentina, 26-28 Feb. 2020. [(SALLUM et al., 2020b)].

E. Sallum, N. Pereira, M. Alves, and M. Santos, "Improving Quality-of-Service in LoRa Low-Power Wide-Area Networks through Optimized Radio Resource Management," *Journal of Sensor and Actuator Networks*, vol. 9, no. 1, pp. 1-26, Mar. 2020 [(SALLUM et al., 2020a)].

1.5.2 Conferences Attended

2020 IEEE International Conference on Industrial Technology (ICIT). Buenos Aires, Argentina, 26-28 Feb. 2020.

1.6 DISSERTATION STRUCTURE

The remainder of the work is structured as follows: Chapter 2 overviews the characteristics of the LoRa communication protocol that are most relevant within the context of this work. Chapter 3 discusses relevant related work.

Chapter 4 presents a method to select radio parameters of LoRa networks, based on a formulation using Mixed-Integer Linear Programming, and the Approximation Algorithm, which can efficiently produce results very close to the optimal. This chapter also presents the simulation setup, the evaluation metrics, and the parameter assignment policies.

Chapter 5 results achieved through the comparative analysis of our parameter optimization method against relevant benchmark policies. Finally, Chapter 6 concludes by summarizing the main contributions and unveiling future research directions.

2 LITERATURE REVIEW

This Chapter presents general aspects of Lora, LoRa physical layer, the device classes of transactions, and the frame structure.

2.1 LORA AND LORAWAN OVERVIEW

LoRa uses a radio frequency technology that allows communication over long distances, with minimal energy consumption and a proprietary Chirp Spread Spectrum physical layer and upper layers defined by an open standard—LoRaWAN. The end-devices can be sensors and actuators, while gateways provide the radio connectivity to end-devices and deliver packets to the network infrastructure composed of network servers and application servers. Network servers are responsible for functions such as checking addresses of end-devices, checking received frames for authenticity, handling acknowledgments, and forwarding application payloads. Application servers perform encryption/decryption of application payloads, manage user authorization, among other related functions (THE THINGS INDUSTRIES, 2019b). Figure 3 shows the LoRaWAN network architecture, composed by end-devices, gateways, network servers, and application servers.

Figure 3 – LoRaWAN network architecture.

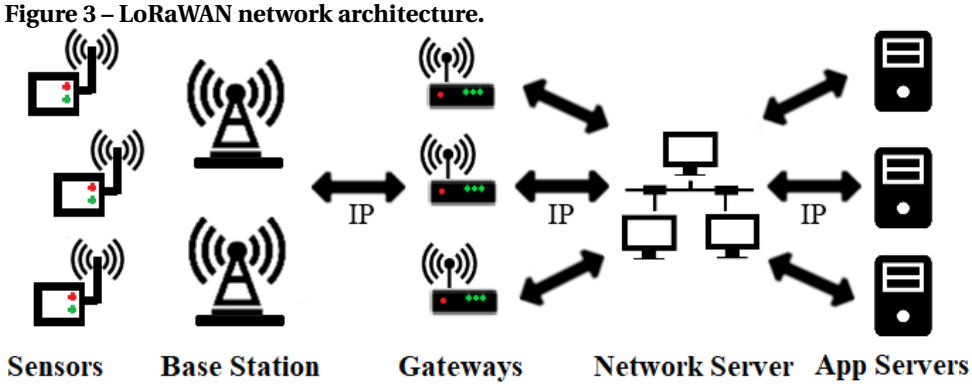

Source: Authorship.

2.1.1 Protocol Stack

Figure 4 shows the LoRaWAN protocol stack.

Figure 4 – LoRaWAN Protocol Stack.

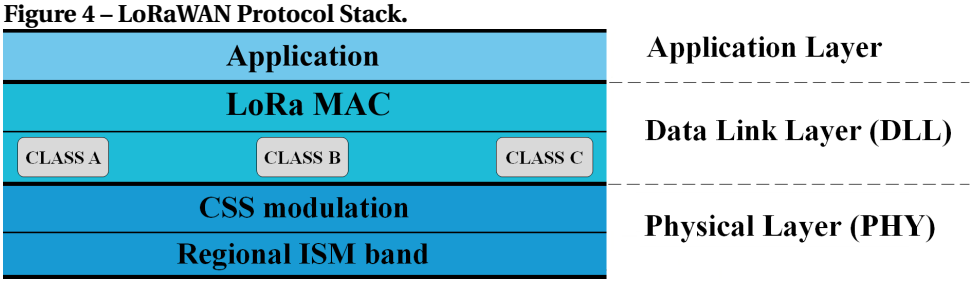

Source: Authorship.

As shown in Figure 4, the top layer is the *Application Layer*. The bottom layer is the *Physical Layer* (PHY), as detailed in Section 2.1.2, responsible for LoRa modulation and ISM band definition, which depends on the geographic region (COMMITTEE et al., 2017). Above the PHY layer, is the *Data Link Layer* (DLL), defined by the LoRa Alliance. To optimize energy consumption, LoRaWAN uses a pure ALOHA (YOUSUF; ROCHESTER; GHADERI, 2018) medium access control mechanism, encompassing three classes of end-devices, namely Classes A–C, as detailed in Section 2.1.3.

2.1.2 LoRa Physical Layer

LoRa has configurable physical layer parameters that control the communication range and throughput as Spreading Factor and Transmit Power to set the modulation rate and the network reach, respectively, coding rate and bandwidth. However, if the N end-devices with the same SF is over one single channel, there will be collisions. The SF impacts time on-air and the distance. Therefore, the higher the value chosen for the SF a more extended range is obtained to the detriment of the data rate.

The airtime of a LoRa transmission is computed according to the payload size and the combination of SF, BW, and CR. These parameters can make the transmission time vary significantly. Table 2 exemplifies the different SNR, airtime, and bitrate resulting from the different SF at a fixed payload length of 20 bytes, $BW = 125$ kHz, and $CR = 4/5$.

Table 2 – LoRa Chirps, SNR, airtime, and bitrate according to parameter SF.

SF	Chirps / Symbol	SNR	Airtime	Bitrate
7	128	−7.5	56.5 ms	5469 bps
8	256	−10	103 ms	3125 bps
9	512	−12.5	185.3 ms	1758 bps
10	1024	−15	371 ms	977 bps
11	2048	−17.5	741 ms	537 bps
12	4096	−20	1318.9 ms	293 bps

Source: Authorship.

The LoRa PHY frequency varies according to regions and is regulated by duty-cycle, bandwidth, and maximum Transmit Power of 14dBM. Sensors located closer to the gateway

can transmit using less airtime and energy. Adjustment of the SF will allow for messages to be transmitted over a greater distance, as shown in Figure 5.

Figure 5 – Ratio between bitrate and Airtime with antenna proximity.

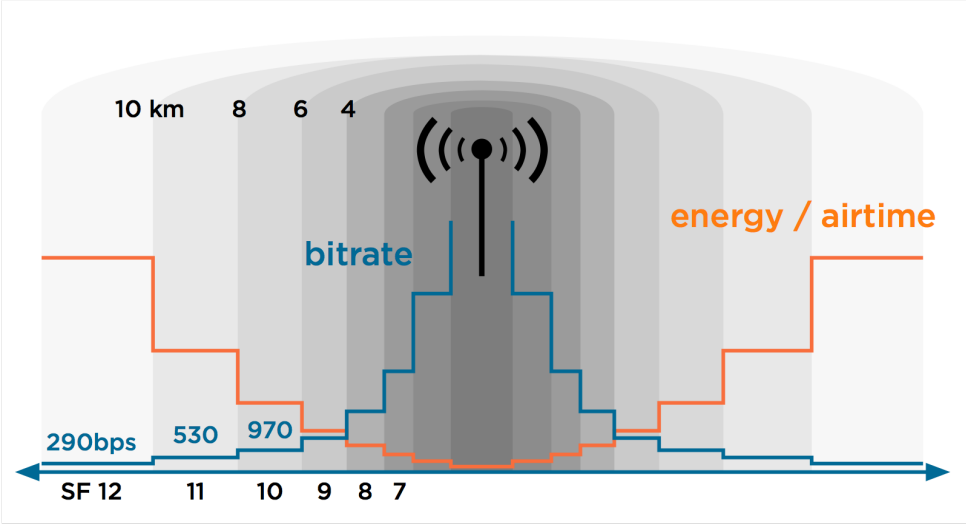

Source: (THE THINGS INDUSTRIES, 2019b).

2.1.3 Class Transactions

The upper layer protocol, LoRaWAN, defines three classes of end-devices, with bidirectional communication, according to downlink latencies and power requirements. Class A devices have longer battery life because of higher latency. The downlink occurs within two windows, both with a specified delay, after an uplink transmission. Figure 6 shows a LoRaWAN Class A transaction.

Figure 6 – LoRaWAN Class A transaction scheme.

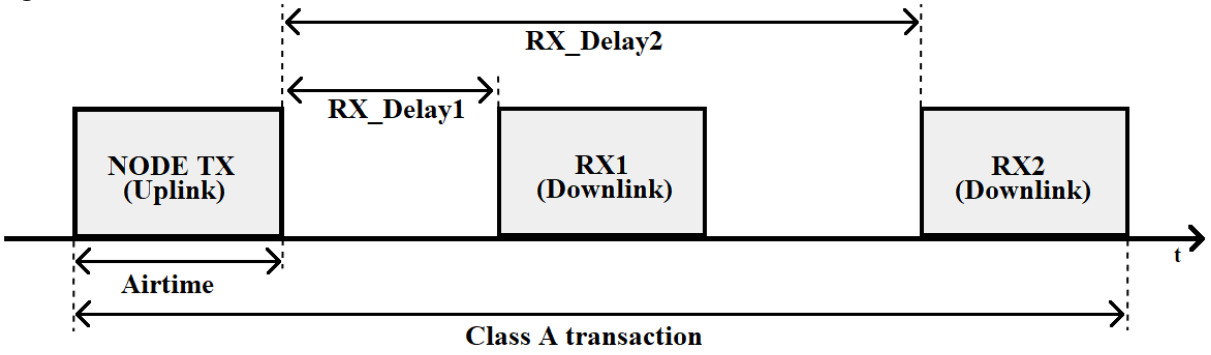

Source: Authorship.

Class B devices schedule downlink receptions from the base station at a pre-established period, determining when applications can send control messages to the end-devices. Concerning Class A, the Class B transaction has additional downlink windows, which occur at specific times following a beacon, as illustrated in Figure 7.

Figure 7 – Class B transaction in up-link direction

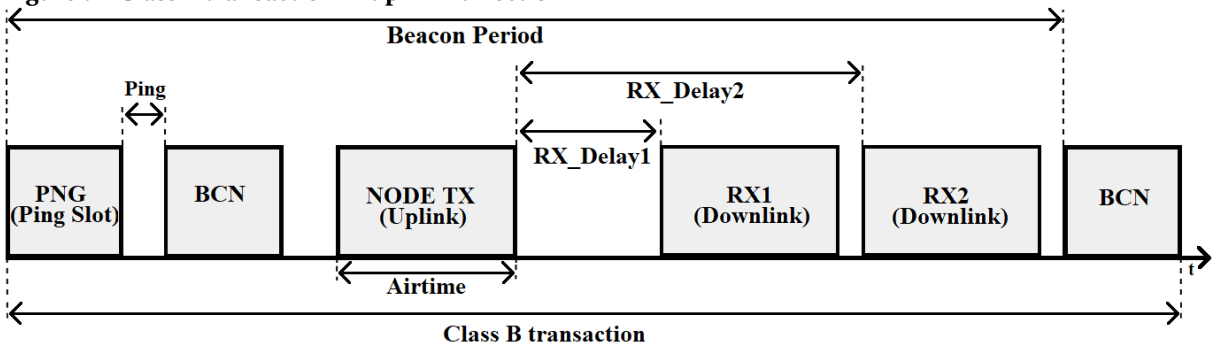

Source: Authorship.

Class C devices are grid-powered and always listening to the transmission medium and thus receive downlink transmissions with the lowest latency (RAZA; KULKARNI; SOORIYABANDARA, 2017). As can be seen in the example shown in Figure 8, it consists of receive windows that remain almost continuously open (only close during transmission).

Figure 8 – LoRaWAN Class C transaction scheme.

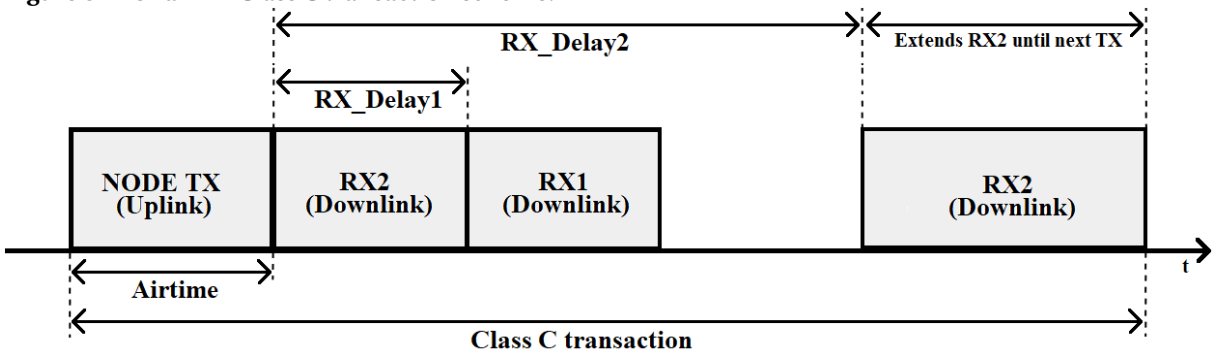

Source: Authorship.

2.1.4 LoRa Medium Access

Low-power sensors transmit the information at low bit-rate asynchronously over a range of kilometers in an industrial environment. e.g., low-power long-distance networks such as LPWAN (XIONG et al., 2015). In these environments, pure ALOHA systems are the best choice for the wide-area random access systems (LoRaWAN) due to the decrease in computer costs caused by data asynchronous. In LoRaWAN, ALOHA manages access to the medium and influence on collisions (RAZA; KULKARNI; SOORIYABANDARA, 2017).

To optimize energy consumption, LoRaWAN uses as channel access mechanism pure ALOHA (YOUSUF; ROCHESTER; GHADERI, 2018). The following example shows the maximum throughput of pure ALOHA in a frame transmitted successfully. G refer to the mean used in the Poisson distribution over transmission-attempt amounts. The set of frame transmission time is T. The probability of there being k transmission-attempts during that

frame-time is:

$$Prob_{1FT} = \frac{G^k e^{-G}}{k!} \tag{1}$$

The average amount of broadcast attempts for 2 successive frame-times is $2G$. Therefore, the probability of successful transmission of a random pair of consecutive frame-times ($Prob_{2FT}$) (KLEINROCK; TOBAGI, 1975) is:

$$Prob_{2FT} = \frac{2G^k e^{-2G}}{k!} \tag{2}$$

Thus, using Poisson distribution, the throughput (S_{pure}) (ABRAMSON, 1970) is expressed by:

$$S_{pure} = Ge^{-2G} \tag{3}$$

A pure ALOHA achieves a maximum throughput, reached when $G = 0.5$, is $0.5/e$ frames per frame-time, of 18.4% of successful transmissions at T. Therefore, the disadvantages of Pure ALOHA is the packet loss and the wastage of time (BAIOCCHI; RICCIATO, 2018).

2.1.5 Frame Structure

The preamble, in a range of 6–65535 symbols, initiates the LoRa packet structure. An optional header, which describes the length and Forward Error Correction (FEC) rate of the payload, specifies a 16-bit Cyclic Redundancy Check (CRC). The header is transferred with a 4/8 FEC rate. Afterward, there is the payload in the packet structure (BOR et al., 2016). Figure 9 shows the frame structure of LoRa.

Figure 9 – LoRa frame structure.

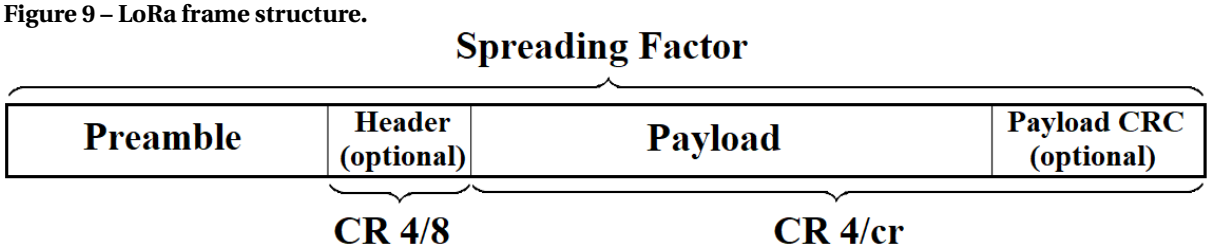

Source: Adapted from (CASALS et al., 2017)

2.1.6 LoRaWAN Adaptive Data Rate

The Adaptive Data Rate (ADR) mechanism is used to optimize the data transmission rate and the transmission power of the network nodes, to optimize network scalability and energy consumption. This mechanism runs asynchronously, with low complexity in the end-devices and with more complexity in the network server. The ADR should only be enabled by

end-devices in stable RF conditions and deactivated when the end-device detect unstable RF conditions. For instance, mobile end-devices must enable the ADR only when they are static for a certain period.

The appropriate data rate is determined by measurements of uplink messages based on the frame counter, SNR, and the number of gateways (THE THINGS INDUSTRIES, 2019d). As specified by the LoRa Alliance Committee et al. (2017), after the ADR bit is set (to 1), the server analyzes the 20 most recent uplinks. If the ADR bit is reset (to 0), the previous measurements are discarded and the measurements start again when the ADR is set again. If uplink messages are not received by the gateway, the ADR algorithm in the end-devices (ADR-NODE) increases the SF value of the subsequent uplink frame, thereby reducing the data rate and increasing the probability of reaching a gateway. Algorithm 1 shows the ADR-NODE algorithm.

Algorithm 1: ADR-NODE (SEMTECH, 2016)

```
ADR_ACK_LIMIT ← 64
ADR_ACK_DELAY ← 32
ADR_ACK_CNT ← 0
if Uplink transmission then
    ADR_ACK_CNT ← ADR_ACK_CNT +1
if ADR_ACK_CNT == ADR_ACK_LIMIT then
    Request response from server
if ADR_ACK_CNT ≥ ADR_ACK_LIMIT + ADR_ACK_DELAY then
    node_SF ← node_SF +1
if Downlink transmission received then
    ADR_ACK_CNT ← 0
```

The server ADR algorithm (ADR-NET) increases the data rate, consequently decreasing the SF, and modifies the TP by measuring the SNR of the received frames, estimated based on the minimum SNR needed for the demodulation, and adjusted according to the specific margin of the device. The new parameters values calculated by the algorithm are sent to the end-device through a downlink frame, to be used in future transmissions (SLABICKI; PREMSANKAR; FRANCESCO, 2018). Algorithm 2 presents the ADR-NET algorithm.

Algorithm 2: ADR-NET (SEMTECH, 2016)

Input : *dataRate*
txPower
SNR
deviceMargin

Output : *desiredDataRate*
txPower

$Link_{margin} \leftarrow$ SNR - demodulationFloor(*dataRate*)
$SNR_{margin} \leftarrow Link_{margin}$ - *deviceMargin*
$nStep \leftarrow SNR_{margin}/3$
$drId_x \leftarrow$ getDataRateIndex (*dataRate*)
for $nStep > 0$ *and* $drId_x < ADR_{MaxDataRate}$ **do**
    $drId_x \leftarrow drId_x + 1$
    nStep $\leftarrow$ nStep -1
for $nStep > 0$ *and* $txPower > txPower_{min}$ **do**
    txPower $\leftarrow$ txPower-3
    nStep $\leftarrow$ nStep -1
for $nStep < 0$ *and* $txPower < txPower_{max}$ **do**
    txPower $\leftarrow$ txPower$+3$
    nStep $\leftarrow$ nStep $+1$

ADR is an important mechanism for optimizing the data transfer rate, airtime, and energy consumption. Understanding its operation is fundamental to make the optimization of radio parameters proposed in this work backward compatible with the standard LoRa protocol (therefore with ADR), as explained in Section 4.2.2. Next, Section 4.1 describes the MILP optimization problem.

2.1.7 Impact Analysis Overhead over LoRa Network

The data rate is the theoretical value that the network can reach since there is no packet loss or interference. In a LoRa network, considering *Spreading Factor*,*Code Rate* and *Bandwidth* as input variables, the data rate is calculated by (SEMTECH, 2019):

$$R_b = SF * \frac{[\frac{4}{4+CR}]}{[\frac{2^{SF}}{BW}]} * 1000 \tag{4}$$

Transmission overhead is the main cause of low performance in the communication link. The right analysis provides designers to establish strategies and algorithms to improve the entire performance and consequently the full better performance of the distributed

computer system. Then, throughput is important and metric to measure how good is the communication and network, i.e., a way to measure the communication performance. The definition of throughput is the amount of data or payload used by applications that are successfully sent/received over the communication link. The measuring unit of throughput can differ from bandwidth due to a range of technical issues, including latency, packet loss, and jitter.

In the LoRa network, for a single user transmitting a data frame, it is used to study the impact of packet transmission overhead on the throughput. If we disregard the propagation times of the signal, then the total time is T_i, where the i is the communication link between base station and node, is expressed in Equation 5:

$$T_i = t_{tr,i} + t_{overhead} \tag{5}$$

, where $t_{tr,i}$ is the data frame transmission:

$$t_{tr,i} = \frac{L}{R} \tag{6}$$

, and t_{overh} is the constant overhead:

$$t_{overh} = t_{preamble} + t_{H,lentgh} + t_{H,cr} + t_{H,crc} + t_{crc} \tag{7}$$

In Equation 6, L is the frame length, and R is the data rate. In Equation 7, $t_{preamble}$ is the inter-frame space. $t_{H,lentgh}$, $t_{H,cr}$, and $t_{H,crc}$ form the header. Moreover, t_{crc} represents the CRC in the physical layer, as shown in Figure 9. Above the MAC layer, the useful throughput is given by (SARKAR, 2011):

$$Throughput = \frac{t_{tr,i}}{T_i} \times \frac{payload}{L} \tag{8}$$

For the throughput analysis of the whole LoRa networks, we have to consider the transmission overhead of each node over the network that measures the overhead of the frame based on Equation 8. Our analysis consists of frames of analyzers with minimum payload and to evaluate the overall performance of the system.

2.1.8 Parameter Assignment Policies

We performed experiments for the following parameter assignment policies:

- ***Min-airtime***: The **min-airtime** is a default assignment used by LoRa end-devices which assigns a fixed CF in CF4 (sub-band g) and SF in SF7 so that packets have the minimum air time (see Table 2). The table in Figure 10 shows an example of allocating SF and CF parameters of **min-airtime** policy on a 96-node LoRa network.

Figure 10 – Example of assignment of min-airtime policy on a 96-node network

	CF1	CF2	CF3	CF4	CF5	CF6	CF7	CF8
SF7	0	0	0	**96**	0	0	0	0
SF8	0	0	0	0	0	0	0	0
SF9	0	0	0	0	0	0	0	0
SF10	0	0	0	0	0	0	0	0
SF11	0	0	0	0	0	0	0	0
SF12	0	0	0	0	0	0	0	0

Source: Authorship.

According to Figure 10, the network nodes were assigned with parameters SF7 and CF4.

- ***Random***: The **random** policy dynamically assigns CF, SF pairs randomly, aiming at reducing concurrent transmissions (that cause packet collision). The table in Figure 11 illustrates an example of allocating SF and CF parameters of the **random** policy in a 96-node network.

Figure 11 – Example of assignment of random policy on a 96-node network

	CF1	CF2	CF3	CF4	CF5	CF6	CF7	CF8	SUM
SF7	5	4	1	1	3	0	2	2	**18**
SF8	3	0	0	2	3	4	2	1	**15**
SF9	0	0	2	3	0	0	4	0	**9**
SF10	4	4	0	3	2	3	0	4	**20**
SF11	3	0	2	4	4	0	2	4	**19**
SF12	1	3	1	0	0	3	4	3	**15**

Source: Authorship.

As shown in Figure 11, the random policy randomly allocated all network nodes between SF1 to SF7 and CF1 to CF8.

- ***Equal-distribution***: With a similar goal to **random**, the **equal-distribution** distributes the number of end-devices equally between CF, SF pairs. The table in Figure 12 shows the example of allocating SF and CF parameters of the **Equal-distribution** policy in a 96-node network.

Figure 12 – Example of assignment of equal-distribution policy on a 96-node network

	CF1	CF2	CF3	CF4	CF5	CF6	CF7	CF8	SUM
SF7	2	2	2	2	2	2	2	2	**16**
SF8	2	2	2	2	2	2	2	2	**16**
SF9	2	2	2	2	2	2	2	2	**16**
SF10	2	2	2	2	2	2	2	2	**16**
SF11	2	2	2	2	2	2	2	2	**16**
SF12	2	2	2	2	2	2	2	2	**16**

Source: Authorship.

According to the table in Figure 12, all SF and CF parameters were assigned equally between network nodes.

- ***Tiurlikova***: The **Tiurlikova** policy is based on the work of Tiurlikova, Stepanov e Mikhaylov (2018), which creates a dynamic allocation method of SF. This policy determines the number of nodes distributed in each SF n_i through Equation (9), where i is the index of SF, T is the airtime (according to Table 2), and N is the nodes numbers:

$$n_i = \frac{\frac{1}{T_i}}{\sum_{i=SF_{\min}}^{SF_{\max}} \frac{1}{T_i}} \cdot N \tag{9}$$

It is important to note that the **Tiurlikova** policy does not specify the allocation of CF parameters. The table in Figure 13 illustrates the example of the allocation of SF and CF parameters of the **Tiurlikova** policy.

Figure 13 – Example of Tiurlikova policy

	CF1 - CF8
SF7	45
SF8	25
SF9	14
SF10	7
SF11	3
SF12	2

Source: Authorship.

According to Figure 13, the **Tiurlikova** policy prioritized the allocation of nodes in SFs that have less air time. 45 nodes were allocated to SF7, 25 to SF8, 14 to SF9, 7 to SF10, and only 3 and 2 nodes were allocated to SF11 and SF12, respectively.

- ***Opt-problem***: The **opt-problem** is the assignment resulting from solving the optimization problem presented using the CPLEX ILP solver (in Section 4.1).

- ***Approx-alg***: The **approx-alg** policy is the result of using the Approximation Algorithm (in Section 4.2). The table in Figure 14 shows the example of allocating SF and CF parameters of policy **opt-problem** and **approx-alg**.

Figure 14 – Example of opt-problem and approx-alg policies on a 96-node network

	CF1	CF2	CF3	CF4	CF5	CF6	CF7	CF8	SUM
SF7	4	2	5	1	1	4	0	3	**20**
SF8	3	2	3	2	1	1	3	0	**15**
SF9	1	3	1	2	2	2	2	0	**13**
SF10	5	2	0	2	0	1	1	2	**13**
SF11	1	2	3	2	2	6	3	2	**21**
SF12	0	2	1	3	5	1	0	2	**14**

Source: Authorship.

According to Figure 14, policies **opt-problem** and **approx-alg** also prioritized the placement of nodes in SFs that have less air time. As the optimization proposed in this dissertation specifies the allocation of the CF parameter, more nodes were allocated to SF7 (SF that has less air time) compared to the Tiurlikova policy.

3 RELATED WORK

Network performance and scalability are key factors for LoRaWAN network design. These factors are influenced mainly by the correct choice of radio parameters and by environmental conditions (RAZA; KULKARNI; SOORIYABANDARA, 2017). Several researchers defined a possible formal approach, through the analysis and comparison of performance and scalability of LoRaWAN networks, for the problem of parameter selection. In this section, we outline some relevant works that address these aspects.

The performance analysis of long-range transmission and channel attenuation, made by Petajajarvi et al. (2015), concludes that, in the best scenario, a single gateway configured using SF 12, 125 MHz BW, and data rate of 1.8 kbps, covers an area of 30 km in peripheral urban environments. Additionally, this paper concludes that low values of SF are recommended for urban scenarios due to less interference caused by the Doppler effect.

In an indoor environment, Neumann, Montavont e Noël (2016) did a performance analysis of the LoRa network with the parameters throughout RSSI, Signal-to-Noise Ratio (SNR), packet loss, packet error, power consumption, and delay to verify how the average current consumption of one end-device impacts in the performance of LoRa network with one device and one gateway. This study concludes that the data rate affects the packet loss.

Bankov, Khorov e Lyakhov (2016) measured the limits of a LoRaWAN network, which is about 0.1 51-byte (Frame Payload) in a network with three main channels and six data rates. That corresponds to 5000 end-devices, each node generating two messages per day. A performance analysis conducted in Mikhaylov, Petaejaejaervi e Haenninen (2016) of LoRaWan end-device using the metrics uplink, throughput, and transmission time concluded that, in terms of LoRaWAN scalability, millions of devices can communicate with a reduced transfer.

Toussaint, Rachkidy e Guitton (2016) evaluated over-the-air performance in a Markov chain model in different traffic conditions, duty cycles, and channel availability. The expected delay and energy consumption of the LoRa network depends on the number of channels, the number of sub-bands, and gateway parameters.

The scalability of LoRaWAN networks evaluated in Abeele et al. (2017) in the ns-3 simulator, in which the error model is based on interference among various concurrent transmissions, concludes that increasing the gateway density improves the negative effect of restrained downstream in packet delivery ratio of upstream messages.

Petäjäjärvi et al. (2017) analyzed the performance of LoRa in three experiments. The first and second experiments were performed in a LoRa end-device under the Doppler frequency shift. With TP of 14 dBm and SF12, at least 60 of the packets are received from 30 km distance on the water. The third experiment was performed on an end-device, mounted in a car, configured with a TP of 14 dBm and SF of 12. This work concludes that, in a mobile scenario, the LoRa communication worsens in a displacement speed of end-devices around

40 km/h.

The work of Vatcharatiansakul, Tuwanut e Pornavalai (2017), in a LoRaWAN performance evaluation, carried out in internal and external environments concludes that the LoRa signal range is affected by the properties of the antennas such as antenna gain, directional, and antenna height.

In the performance analysis of LoRa network performed in Vangelista (2017), with Additive white Gaussian noise (AWGN), a frequency selective channel of the Frequency Shift Chirp Modulation (FCSM), and the Frequency-Shift keying modulation (FSK), the authors concluded that the performance of the FCSM and FSK in an AWGN channel are equivalent. However, in a frequency selective channel, the FCSM has a superior performance.

The work of Cattani, Boano e Romer (2017) presents an analysis of the performance of the LoRa about different configurations of PHY and environmental conditions. The analysis done in a scenario where the network nodes are at the communication limit concludes that it is more efficient to use the faster PHY configuration and higher transmission power than slower configurations that maximize the quality of the link because the faster PHY setting provides 100 times faster effective bit rate than the slower setting scenario, at the cost of a 10% lower average packet reception rate. Also, the work concludes that environmental factors such as temperature and humidity impact the rate of reception of packets and the intensity of the received signal. In a controlled environment with a temperature of 15 °C, an optimal link with 100% Packet Reception Rate becomes unusable at 60 °C. Over this temperature range, the received signal strength is reduced by 6 dBm, being 1 dBm per 10 °C.

Yousuf, Rochester e Ghaderi (2018) measured how internal and external urban environments affect the LoRa signal. In an internal environment of a seven-story building, there was a minimal packet drop. The external coverage depends on the environment. In this experiment performed in a range of 4.4 km, there was 15% of packet drops and the packet size alter the signal range.

Reynders et al. (2018) analyzed and compared the performance of LoRa networks with a proposed MAC layer two-step lightweight scheduling in the ns-3 simulator. The results conclude that in a scenario with one gateway and 1000 end-devices, the proposed MAC layer reduces the Packet Error Ratio around 20%.

Lim e Han (2018) made a proposal and schema validation to maximize the average Packet Success Probability through SF parameters using MATLAB simulator on Massive Connectivity (MC), respectively. The projected scheme is better for all others MC to Monte Carlo simulations and analysis. For example, in a 2000 end-devices LoRa network, the method provides stability for 810 end-devices, an increase of 22% in MC over the Equal-Area-Based scheme.

Feltrin et al. (2018) characterized experimentally from the link-level viewpoint and evaluated through simulations the capacity of a LoRaWAN gateway to provide communica-

tions in large rural environments. In this scenario, a gateway covering an area of 1 km^2, the maximum node density is 185 end-devices/hectare. However, using this gateway in an area of 46.5 km^2, the maximum density decreased to one node/hectare. To maximize the node density in this large area, four gateways provide 40 end-devices/hectare.

In Tiurlikova, Stepanov e Mikhaylov (2018), the authors proposed an optimized SF parameter allocation approach, stating that it increases the probability of uplink data delivery by 20–40% at the cost of increased power consumption by 1–8%, respectively. Due to its relevance in the context of this paper, we considered this algorithm as a benchmark (dubbed "Tiurlikova") in the comparative performance analysis outlined in Section 4.3.

The work of Zorbas e O'Flynn (2019) proposes a collision-free scheduling approach in which each node autonomously decides when to transmit a packet based on its unique identifier. The frame size, the execution time of the exhaustive search, and the collision rate are evaluated in this work using the LoRasim simulator in scenarios of up to 300 network nodes. In the evaluated network scenarios, the proposed approach obtained a collision rate between 4–35%, a lower rate compared to the native LoRa, which obtained a collision rate between 9–48%. The proposed approach provides high reliability when nodes are synchronized over networks with a low number of nodes.

In the work of Lee e Youn (2020), the objective is to propose a group-based transmission scheduling scheme (GTSS) to solve the problem of building a massive IoT network of LoRa devices. The evaluation metric used is LoRaSim. With a number of network nodes between 20,000 and 120,000, each device sends a message to the gateway once a day. The work concludes that it is possible to build a massive IoT network of LoRa devices. The proposed GTSS achieved high data delivery stability in massive IoT environments, with a value Packet Delivery Rate 5%–10% higher than the LoRa standard.

Differently from the studies presented, this work proposes to optimize the performance of LoRaWAN networks through a dynamic assignment policy of SF and CF parameters, which is backward compatible with the standard protocol and ADR mechanism. The proposed policy was compared and analyzed against LoRaWAN's default assignment policy, and the random, Tiurlikova's, and equal dynamic assignment policies.

4 METHODOLOGY

This chapter describes the methodology used for the development of this work. Figure 15 presents the flowchart of the process stage of the work proposal.

Figure 15 – Process stages flowchart.

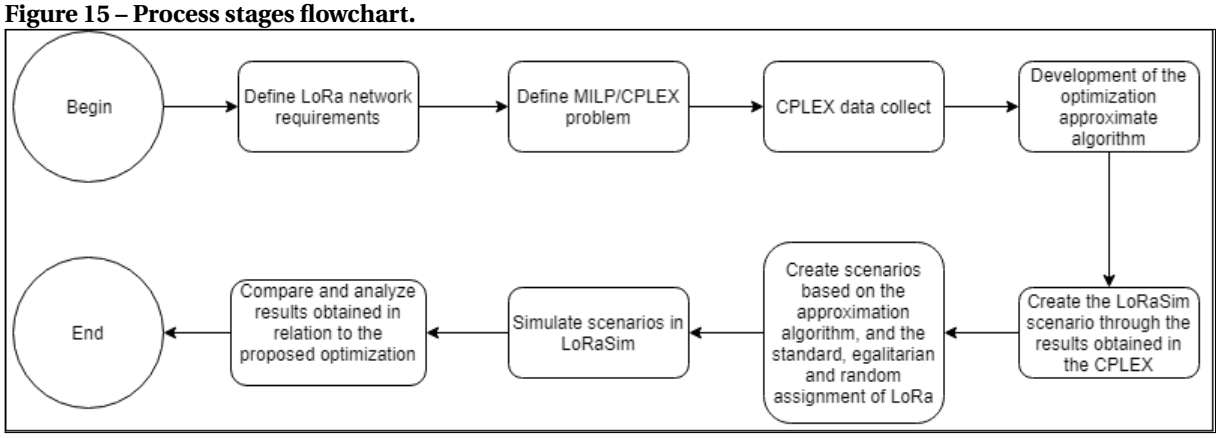

Source: Authorship.

Following the steps described in Figure 15, Section 4.1 present a method to select optimal values to CF and SF radio parameters, based on a formulation using *Mixed Integer Linear Programming*. Section 4.2 presents the Approximation Algorithm, which can efficiently produce results very close to the optimal. Finally, Section 4.3 outlines the simulation setup, the evaluation metrics, and the parameter assignment policies.

4.1 MILP OPTIMIZATION PROBLEM

To increase the performance of the LoRaWAN network through the optimization of radio parameters, we developed a formulation using *Mixed Integer Linear Programming* (MILP), a formal mathematical optimization framework. Using MILP provides a mathematical framework that allows solving complex problems by leveraging well-established theory and solution methods. Similar approaches using a MILP formulation in-network parameter optimization scenarios can be found in previous work (e.g., Gounaris et al. (2016), Samsatli e Samsatli (2018)). It is also important to note that the optimization problem is the baseline for the approximation algorithm, allowing us to benchmark the approximation against an optimal solution.

Many objectives can be selected to improve the performance of LoRaWAN networks, e.g. reduce the individual node energy consumption, improve the reliability of data delivery, or improve overall throughput. For this work, we aim to minimize the number of collisions and energy consumption of the Lora network by setting the radio parameters of the LoRaWAN devices in the network. Our performance problem for LoRaWAN, modeled as a MILP problem,

assigns values to the CF and SF parameters to improve the performance of the network. Section 4.1.1 presents general aspects of the MILP, Section 4.1.2 introduces the notation and model used, and Section 4.1.3 presents our MILP problem formulation.

4.1.1 Background on Mathematical Optimization

Mathematical optimization has been used in a great number of fields, such as in Earl e D'Andrea (2005) for vehicle- control problems, in Méndez, Henning e Cerdá (2001) for short-term scheduling of resource-constrained multistage flow-shop batch facilities, in Borghetti et al. (2008) for short-term hydro scheduling and unit commitment with the head-dependent reservoir, and in Richards e How (2002) for aircraft planning with collision avoidance. Mathematical optimization is also used for automotive applications when optimizing extensibility Zhu et al. (2010) or task activation modes Zheng et al. (2007). The problems can be expressed by a set of integer, binary and continuous design variables, design parameters, linear equalities and inequalities representing the constraints on the solution, and a linear objective function. The main advantage consists in the possibility of leveraging a well-established theory and solution methods, which includes the availability of efficient solver engines with controllable solution accuracy and constrained computing time (BORGHETTI et al., 2008).

Linear Programming is a method for solving design problems using the formal mathematical optimization framework. A MILP optimization problem is given for a set of variables, objective function, and a set of constraints. Solving the problem attempts to find the best solution for the objective function in the set of solutions that satisfies the constraints. A MILP problem is given in the form $\min_x cx$, subject to $Ax \leq b$, where $x \in Z^n \times R^p$. In Integer Programming Problem, all variables are limited to be an integer. The set S of $x \in Z^n \times R^p$ which satisfy the linear constraints $Ax \leq b$ is the Feasible Set:

$$S=\{x \in Z^n \times R^p, Ax \leq b\} \tag{10}$$

An element $x \in Z^n$ is the feasible solution. The optimization problem finds a solution in the feasible set that yields the best objective value, a feasibility problem finds an element that satisfies all constraints and restrictions,i.e., find an element in the feasible set.

4.1.2 Notation and Model

Consider a wireless network system with a LoRaWAN gateway and n end-devices. End-devices transmit with an average transmission rate λ packets/second and an average length of ξ bytes. The time to transmit a packet of length ξ is given by a function $airtime(\xi, cf)$,

which computes the time to transmit according to parameters SF, CR, BW, and payload size. For this model, we assume a fixed BW and CR, which must be taken into account for the airtime computations.

To model our problem as an MILP problem, we define an array of tuples $R_{i\in\{i\ldots n\}} = \left(cf_{i,CF}, sf_{i,SF}\right)$ for each end-device, where CF is a list of available CFs and SF is a list of available SFs. The lists of SFs and CFs as input allow, e.g., reserving certain CF for other uses. An example input could be $CF = 868.1, 868.3, 868.5$ and $SF = 7, 8, 9, 10, 11, 12$ indicating that the algorithm can use three CFs (868.1, 868.3, and 868.5) and 7–12 SFs in each of these channels. The $\left(cf_{i,CF}, sf_{i,SF}\right)$ tuples are arrays of booleans which indicate if an end-device i is using a given CF or SF. These are the decision variables of our problem and one of the constraints of our model must restrict the solutions to only having one value of each of the arrays set to true in each end-device, as each end-device can only have one CF and one SF value assigned. Figure 16 illustrates the example of LoRa devices and the respective decision variables connected to the gateway

Figure 16 – Example of LoRa device decision variables

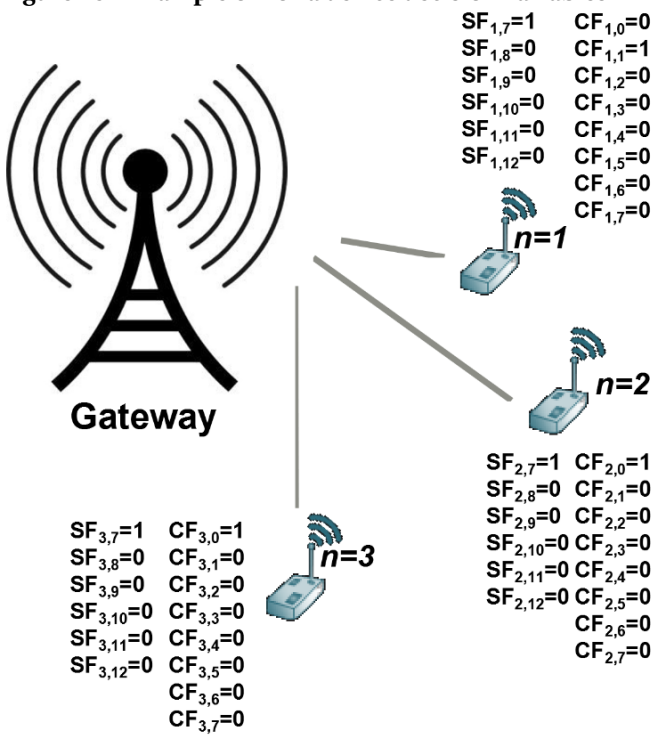

Source: Authorship.

The end-devices of the LoRaWAN networks as $N = \{N_1, N_2, N_3 \ldots N_n\}$ with CF and SF parameters communicate with gateway G. To increase network performance, multiple indexes are considered: energy consumption of the end-devices, network range, interference reduction, and errors rate. In this case, CF and SF are assigned to maximize the probability of success on a single gateway. As an input, to model the LoRaWAN network as MILP, we are given variables $\forall_i \in \{1 \ldots N\} CF_n, SF_n$ where N is equal to the number of end-devices.

4.1.3 MILP Problem Statement

Considering that SFs are orthogonal with each other, we want to minimize the collision probability for each CF, SF pair. Therefore, the decision variables for each node have two Boolean arrays CF_n and SF_n that indicate the CF and SF of each N. For example, the following arrays indicate that N_1 is using CF_7 and CF_1:

$$\begin{aligned} SF_{1,7} &= 1 & CF_{1,0} &= 0 \\ SF_{1,8} &= 0 & CF_{1,1} &= 1 \\ SF_{1,9} &= 0 & CF_{1,2} &= 0 \\ SF_{1,10} &= 0 & CF_{1,3} &= 0 \\ SF_{1,11} &= 0 & CF_{1,4} &= 0 \\ SF_{1,12} &= 0 & CF_{1,5} &= 0 \\ & & CF_{1,6} &= 0 \\ & & CF_{1,7} &= 0 \end{aligned}$$

To express this in our MILP model, we define in Equation (11) the following objective function, which minimizes the difference between the utilization of each CF, SF pair, denoted as $U_{cf,sf}$, resulting in the minimum load for each CF, SF:

$$\sum_{cfi \in CF} \sum_{sfj \in sf} \left(U_{cfi,sfj} - U_{cfl,sfk}\right) \tag{11}$$
$$cfl : cfl \in CF \wedge cfi \neq cfl;$$
$$sfk : sfk \in SF \wedge sfj \neq sfk;$$

where

$$U_{cfi,sfj} = N_{cfi,sfj} \times airtime(\xi, sfi) \times \lambda; \tag{12}$$
$$U_{cfl,sfk} = N_{cfl,sfk} \times airtime(\xi, sfk) \times \lambda$$

and

$$N_{cfi,sfj} = \sum_i^n cf_{i,cfi} \times sf_{i,sfj} \tag{13}$$
$$N_{cfl,sfk} = \sum_i^n cf_{i,cfl} \times sf_{i,sfk}$$

subject to

$$\sum_{cf \in CF} \left(cf_{i,cf}\right) = 1 \quad \forall i : 1..n \tag{14}$$

and

$$\sum_{sf \in SF} \left(sf_{i,sf}\right) = 1 \quad \forall i : 1..n \tag{15}$$

Equation (12) computes the utilization of the CF, SF pair, as defined by Equation (13), considering the number of end-devices assigned to that pair. The two constraints in Equations (14) and (15) limit the assignment CF and SF such that each end-device is only assigned one CF and one SF.

Practical Issues: Equation (13) is the product of two binary variables, which is nonlinear. This can however be made linear given

$$z_{i,cf,sf} = cf_{i,CF} \times sf_{i,SF} \tag{16}$$

and the following additional constraints:

$$z_{i,cf,sf} \leq cf_{i,cf} \tag{17}$$

$$z_{i,cf,sf} \leq sf_{i,cf} \tag{18}$$

$$z_{i,cf,sf} \geq cf_{i,cf} + sf_{i,cf} - 1 \tag{19}$$

This problem can be solved using one of the many state-of-the-art MILP solvers. In our experiments, we used the CPLEX optimizer (IBM, 2019) due to the set of different options, strategic decomposition, and deactivation of heuristics that reduce the time to solve complex problems (LIMA; GROSSMANN, 2011).

4.2 APPROXIMATION ALGORITHM

The ADR mechanism, as described in Section 2.1.6, improves the data rate, airtime, and power consumption of each end-device through the TP and SF parameters according to SF, TP, BW, and SNR. However, the performance of a LoRaWAN network also depends on the occurrence of simultaneous transmissions with the same SF, determined through the two-dimensional coordinates of the end-devices and the LoRaWAN network gateways.

To apply the results obtained through the MILP problem formulation, as described in Section 4.1.1, with backward compatibility in LoRaWAN networks, we rely on the ADR mechanism to dynamically adjust the settings of end-devices. As indicated by the standard, only end-devices with a stable RF environment should enable ADR. Our model includes provisions for defining a list of end-devices for which the SF parameter, determined by measurements (which are part of the normal LoRaWAN ADR procedure), can be changed. This is backward compatible with existing LoRaWAN networks and only the LoRa network server needs to be updated to obtain the radio parameters according to our proposed method.

4.2.1 Description of the Approximation Algorithm

The time to solve MILP problems grows exponentially as the number of end-devices increases. Due to scalability issues, we developed the Approximation Algorithm to provide parameter assignments (Algorithm 3). The approximation is based on a first-fit assignment of the utilization for each CF and SF combination.

Algorithm 3: Approximation Algorithm.

Input : ξ, the average packet length in bytes
λ, the average packet transmission rate
Array CF of available CFs
Array SF of available SFs, sorted by airtime

Output : Array R of (cf_i, sf_i) tuples with the CF and SF settings for node i

forall *elements of* CF **do**
  forall *elements of* SF **do**
    $U_{cf,sf} \leftarrow 0$

forall *elements of* V **do**
  $R_i \leftarrow mincfsf(U)$; ▷ (cf_i, sf_i) tuple
  $U_{R_i} \leftarrow U_{cf,sf} + \frac{airtime(\xi, sf_i)}{1/\lambda}$

The Approximation Algorithm in Algorithm 3 receives as input the average packet length in bytes (ξ), and the average packet transmission rate (λ). It also receives two arrays with the available CFs and SFs, with the SF array being ordered from the SF with the smallest resulting airtime to the largest.

Algorithm 3 starts by creating an array of $U_{cf,sf}$ to hold the utilization of each (CF, SF) pair. Then, the algorithm assigns a CF and SF to each end-device by using a $min_{cf,sf}(U)$ function which takes as input the array $U_{cf,sf}$ and returns a (cf_i, sf_i) tuple that will result in the lowest utilization increase. That is, it will return the CF, SF pair that is the $min(U_{cf,sf} + airtime(\xi, sf)) \forall sf : sf \in SF$. Finally, the algorithm increases the utilization for that CF, SF pair.

4.2.2 Backward Compatibility with LoRaWAN

The LoRa Server project provides a set of open-source applications for building LoRaWAN networks. It is part of a larger project that encompasses a protocol packet forwarder broker for MQTT (LoRa Gateway Bridge), and a compatible application server. The mechanisms provided by LoRa Server allow users to manage the gateways in the LoRa network, the

supported applications, and the devices associated with the applications (LORA SERVER,).

Reviewing the documentation for sending LoRa server uplink messages (THE THINGS INDUSTRIES, 2019a; LORA ALLIANCE, 2019), the way to implement the Approximation Algorithm with backward compatibility with the standard LoRa protocol and its mechanisms, e.g., ADR (as described in Section 2.1.6), is to implement the Approximation Algorithm at the LoRa application layer of LoRa and devices. Thus, the application layer determines the CF, SF pair individually for each node. The LoRa Server receives as input parameters the CF, SF pairs by the application server (that is running the Approximation Algorithm) and transmits to the end-devices in the downlink. Then, the node executes a corresponding application to configure the node parameters.

4.3 EVALUATION

To study the performance of different parameter selection strategies, including the ones assigned by solving the optimization problem presented in Section 4.1 and the algorithm in Section 4.2, we carried out a simulation study based on the tools developed in Bor et al. (2016). We aimed at studying the scalability of the network, namely analyzing different performance metrics according to the number of end-devices and topologies. Building and analyzing such LoRaWAN networks would be infeasible in practice, so we opted to base our study in simulation.

Experiments were run on a Linux server with Ubuntu 16.04.4 LTS operating system with Intel Xeon E5-2637 processor running at 3.50GHz using 64 GB of RAM.

4.3.1 Simulation Setup

The LoRa simulation tool, *LoRaSim*, allows defining model LoRa networks by setting the number of end-devices inserted in a two-dimensional area, average packet transmission rate (Λ), the number of base stations and other radio parameters such as SF, CR, and BW (BOR et al., 2016). However, *LoRaSim* does not consider channel hopping and downlink messages.

SFs are imperfectly orthogonal. However, for traceability purposes, in our experiments, we assumed that a single base station can simultaneously decode concurrent signals on all orthogonal SF and BW settings. This assumption can be supported in practice with multiple LoRa chips, such as the ® SX1301 (SEMTECH, 2017b). In our simulations, it was considered that the RF is stable and the network devices are fixed. Table 3 presents the simulations parameters common to all simulation runs.

Table 3 – Simulations parameters.

Parameter	Value
Code Rate (CR)	4/5
Bandwidth (BW)	125 kHz
Sub-band	g and g1
Transmission Power (TP)	14 dBm
Number of base stations	1
Transmission range	99 and 350 m
Payload size ξ	20 bytes
Average packet transmission period	16.6 min
Scenario run time	1 year
Node distribution	Randomly distributed
Traffic Model	Poisson distribution model
Propagation Model	Log-distance path loss model
End-device operating voltage	3 V
Device Class	Class A

Source: Authorship.

According to Table 3, the simulated scenarios run time was one year, with all devices transmitting data at an average send interval of 16.6 min. This means that each end-device transmitted 86 times a day within one year. We run 30 simulations for each scenario variation, each with a random uniform node distribution in space.

Also, the reason for the chosen transmission distance, 99 and 350 meters are to represent applications where there are many LoRa devices in a restricted space. For example in buildings and condominiums, where LoRa technology can be applied to water and energy meters, temperature sensor, parking presence sensor, smoke detectors, etc (KHUTSOANE; ISONG; ABU-MAHFOUZ, 2017). Figure 17 shows a network scenario created with the parameters shown in Table 3.

Figure 17 – Network scenario created with a transmission range of 99 meters. The black dot represents the gateway.

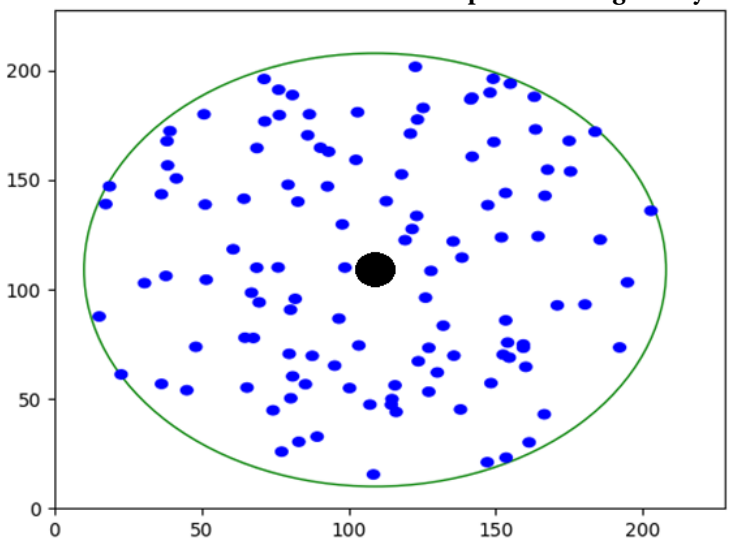

Source: Authorship.

4.3.2 Evaluation Metrics

We used three evaluation metrics to evaluate the performance of a LoRaWAN network as follows: *Data Extraction Rate*, *number of collisions*, and *Network Energy Consumption* (NEC).

Data Extraction Rate provides a network-wide measure of the valid packets received in a numerical range between 0 and 1, wherein for optimal network deployments the value is equal to 1. Equation (20) shows how the DER can be computed, where Nr represents the number of packets received, C the number of packet collisions, and Ns the total number of packets sent.

$$DER = \frac{Nr - C}{Ns} \tag{20}$$

The *number of collisions* provides further insight into the changes in the DER. Packet collisions occur when two or more network nodes attempt to send data simultaneously, resulting in collisions and possible loss of transmitted data, harming system performance. When two LoRa transmissions occur at the same time (perceived at the receiver), it is determined that the receiver can decode received packets simultaneously by analyzing CF, SF, energy, and time conditions. The collision behavior evaluated in *LoRaSim* simulations depends on the following parameters:

- **Reception overlap:** In *LoRaSim*, two packets overlap when the reception intervals overlap. It is represented by $O(x, y)$.
- ***Carrier Frequency***: It is evaluated whether transmissions with the same CF and BW parameters but different SFs can be successfully decoded. Importantly, they are available assuming two reception paths. CF collision is expressed by $C_{CF}(x, y)$.
- ***Spreading Factor***: Transmissions with different SF (and same CF and BW) can thus be successfully decoded. SF collision is expressed by $C_{SF}(x, y)$.
- **Power (capture effect):** In our simulations, the capture effect was considered, which is modeled on *LoRaSim* to match a ® SX1272. It is defined when two signals occur simultaneously at the receiver and the weakest signal is suppressed by the strongest. It is determined by $C_{pwr}(x, y)$.
- **Timing:** Experiments conducted by Bor et al. (2016) conclude that packages can overlap as long as there are at least five preamble symbols intact. This defines the transmission interval that two transmission packets collide within their critical section. It is represented by C_{timing}.

Given these parameters, *LoRaSim* assumes that two packets x and y collided if Equation (21) is true:

$$C(x,y) = O(x,y) \wedge C_{CF}(x,y) \wedge C_{SF}(x,y) \wedge C_{pwr}(x,y) \wedge C_{timing}(x,y) \tag{21}$$

More information on collision behavior in LoRa can be found in Bor et al. (2016).

Network Energy Consumption (NEC) is defined as the energy spent by the network to extract a message successfully, considering all network nodes. It depends on parameters such as SF, BW, CR, and TP. By definition, the NEC metric evaluates the network as a whole, not just individual node behavior, and grows proportionally as the number of end-devices increases. A low value of NEC means that the network parameters have been set efficiently (VOIGT et al., 2017). Equation (22) describes the calculation of NEC in Joules, where V is the operating voltage, defined as 3 V according to Table 3. Ns is the total number of packets sent, i is the end-device index, TX is the transmission power consumption of each end-device in mA, and $airtime$ depends on the parameters SF, CR, BW, and payload size of each end-device.

$$NEC = \sum_{i=0}^{n} (airtime_i * (TX_i)) * V * Ns \tag{22}$$

5 RESULTS AND DISCUSSIONS

This chapter shows the results and discussions obtained in this work. Section 5.1 shows a network scalability analysis obtained by the assignment policies (see Section 2.1.8). Section 5.2, 5.3, and 5.4 show the results obtained from *DER*, *number of collisions*, and *Network Energy Consumption*, respectively.

Section 5.5 shows the analysis and comparison of the ADR mechanism, described in Section 2.1.6, in the **approx-alg** and **random** assignment policies. Section 5.6 analyzes the Lora data rate, analyzing and comparing the theoretical throughput of the standard protocol with other assignment policies. Finally, Section 5.7 shows the analysis of the circumstances brought about by the optimization proposed in the standard Lora protocol.

5.1 ANALYSIS OF NETWORK SCALABILITY OF ASSIGNMENT POLICIES

According to the ETSI EN300.220 standard, in Europe, the max-duty-cycle for g (863.0–868.0 MHz) and g1 (868.0–868.6 MHz) bands is 1% (see Table 1). The limit of utilization of these subbands is represented mathematically by Equations (23) and (24), where i is the index of each node, T is the airtime (according to Table 2), and N is the nodes numbers:

$$sum_{n\in\{1..N\}} \sum_{cf=\{CF4,CF5,CF6,CF7,CF8\}} \sum_{sf=\{SF7,..,SF12\}} (CF_{i,cf}.SF_{i,sf}.T_{SF} * \Lambda) \leq 0.01 \tag{23}$$

$$sum_{n\in\{1..N\}} \sum_{cf=\{CF1,CF2,CF3\}} \sum_{sf=\{SF7,..,SF12\}} (CF_{i,cf}.SF_{i,sf}.T_{SF} * \Lambda) \leq 0.01 \tag{24}$$

Considering a network scenario with the configuration parameters in Table 3, Table 4 shows the maximum number of nodes that can be allocated for each assignment policy, resulting from calculating the sub-band use of each pair of CF, SF through Equations (23) and (24).

Table 4 – Network scalability according to allocation policy.

Policy	Sub-Bands	Maximum Number of Nodes
equal-distribution	g and g1	72 nodes
Tiurlikova	g and g1	128 nodes
min-airtime	g or g1	176 nodes
random	g and g1	353 nodes in best-case
opt-problem/approx-alg	g and g1	353 nodes

Source: Authorship.

The results in Table 4 show that the policies that best scaled the network are **opt-problem** and **approx-alg**. This is due to the optimization to dynamically assign to each node

the (CF, SF) pair leading to the shortest airtime, considering the use of sub-bands g and g1. As a result, the **opt-problem** and **approx-alg** policies allow the best scaling of the network, with a maximum number of 353 nodes. The **Tiurlikova** allocates 64 nodes per sub-band. Using sub-bands g and g1, the number of nodes that can be allocated is 128.

In the best-case scenario, the maximum number of nodes that can be allocated with the **random** policy is 353 nodes if the randomly generated CF and SF values for all nodes are the same as **opt-problem** and **approx-alg** policies (regardless of their ordering). However, the **random** policy allows only six nodes to be allocated in the worst-case scenario, which is all nodes allocated in SF12 using only one of the sub-bands (g or g1).

The **min-airtime** assignment policy allocates a maximum of 176 nodes, respecting the max-duty- cycle limit of 1%, with all nodes configured in SF7 using the g sub-band. Importantly, policy **min-airtime** uses only the sub-band. If sub-band g1 is enabled, network scalability results are similar to **opt-problem** and **approx-alg** policies, with 353 nodes. Finally, the maximum number of nodes that can be allocated with the **equal-distribution** policy is 66 nodes.

To represent the difference between assignment policies, the network scenarios used in our simulations range up to 1500 nodes with no duty-cycle restrictions. The chosen transmission range is 99 m radius, which represents a transmission range in built environments, and 350 m radius, a range chosen due to the limitation of the min-airtime policy (which uses SF7) based on the experiments performed with the simulation parameters in Table 3.

5.2 DER

Figure 18 shows the results of DER as a function of the number of end-devices with a gateway transmission range of 99 m radius.

Figure 18 – DER as a function of the number of nodes in the 99 m radius scenario.

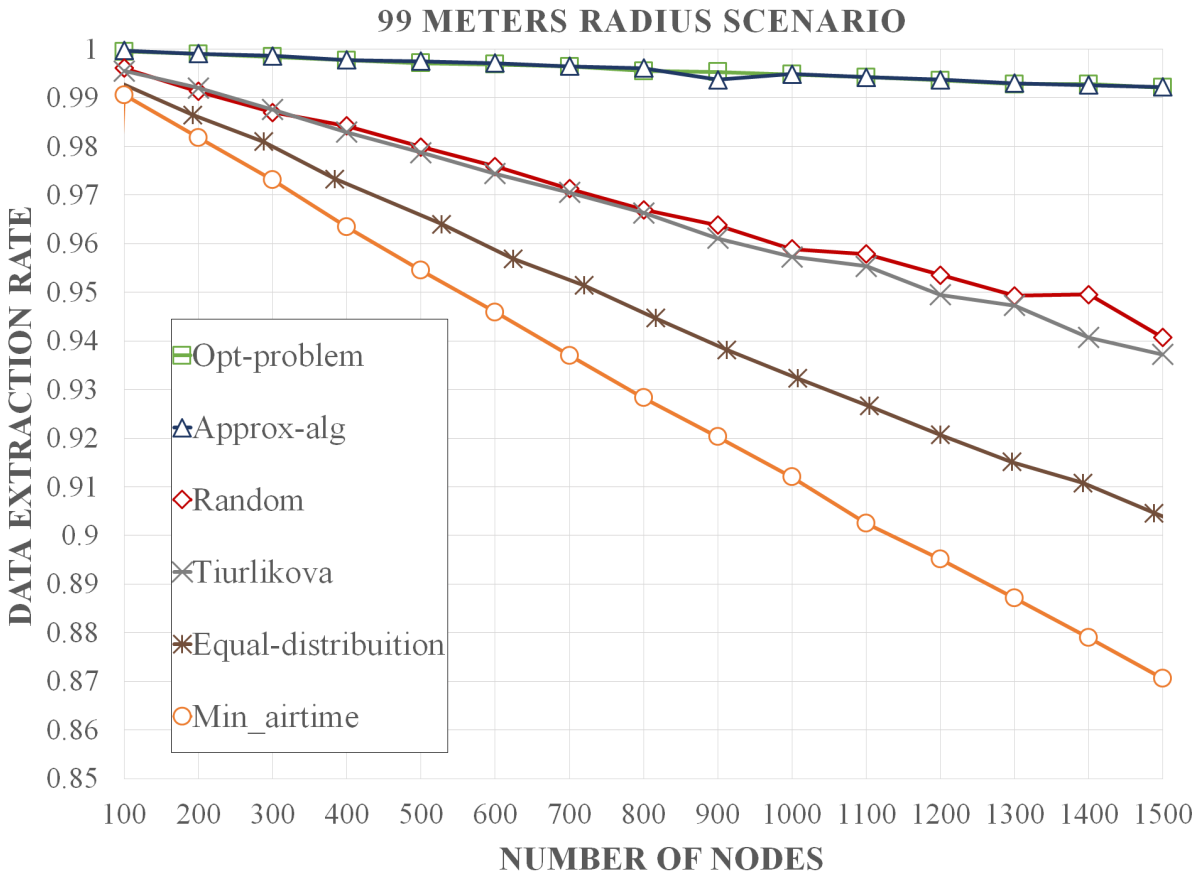

Source: Authorship.

As shown in Figure 18, the policies **opt-problem** (green line) and **approx-alg** (navy blue line) show the highest DER performance with an average increase of 7.14%, 5.19%, 3.03%, and 2.82% in relation to the **min-airtime** (orange line), **equal-distribution** (brown line), **Tiurlikova** (silver line), and **random** (red line), respectively.

Figure 19 presents the results of DER as a function of the number of end-devices with a gateway transmission range of 350 m.

Figure 19 – DER as a function of the number of nodes in the 350 m radius scenario.

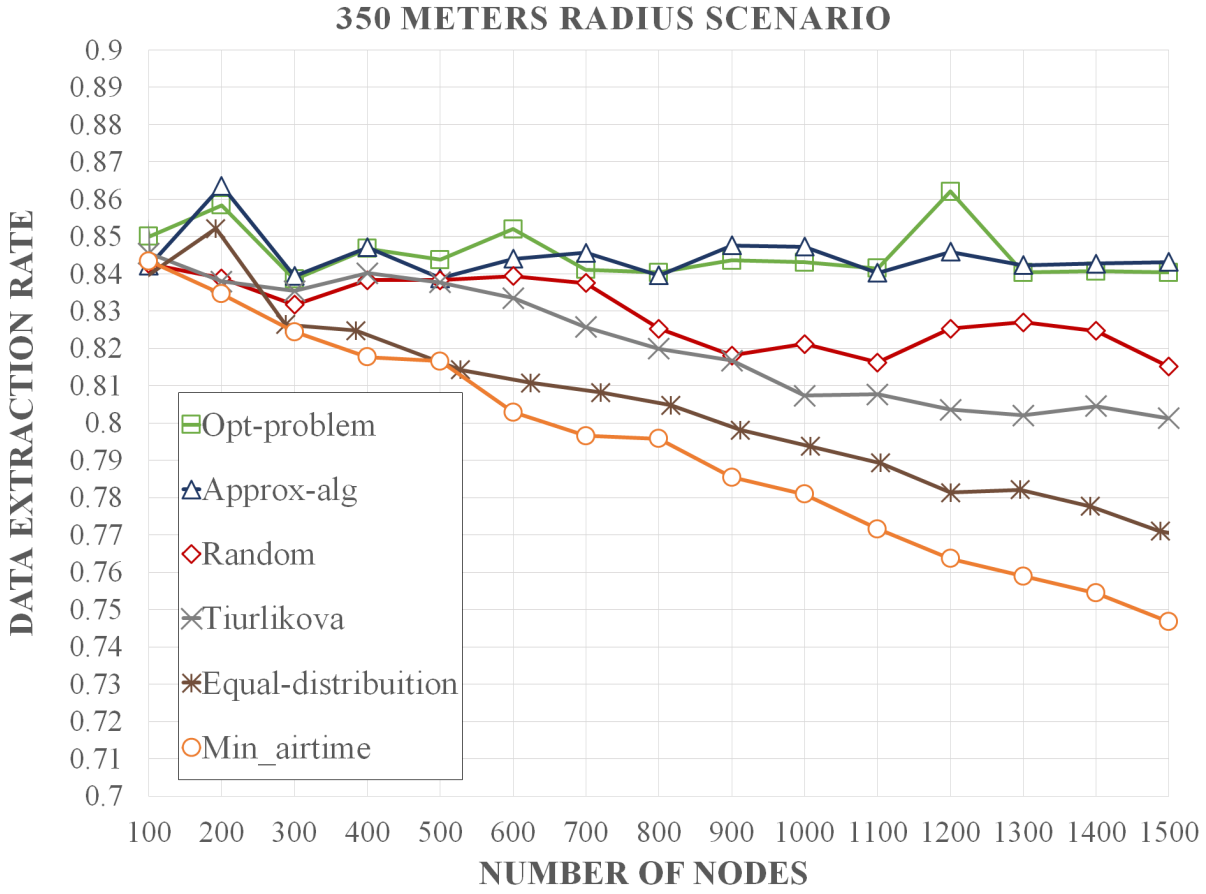

Source: Authorship.

According to Figure 19, the **opt-problem** shows the highest DER performance with an average increase of 6.63%, 5.04%, 2.95%, 1.95%, and 0.1% in relation to the **min-airtime**, **equal-distribution**, **Tiurlikova**, **random**, and **approx-alg**, respectively.

Figures 18 and 19 show that, as the number of nodes increases, the DER value decreases. This demonstrates how increasing the number of nodes affects the performance of LoRa networks.

5.3 *NUMBER OF COLLISIONS*

Figure 20 illustrates the *number of collisions* according to the number of nodes with a gateway transmission range of 99 m radius.

Figure 20 – Number of collisions according to the number of nodes in the 99 m radius scenario.

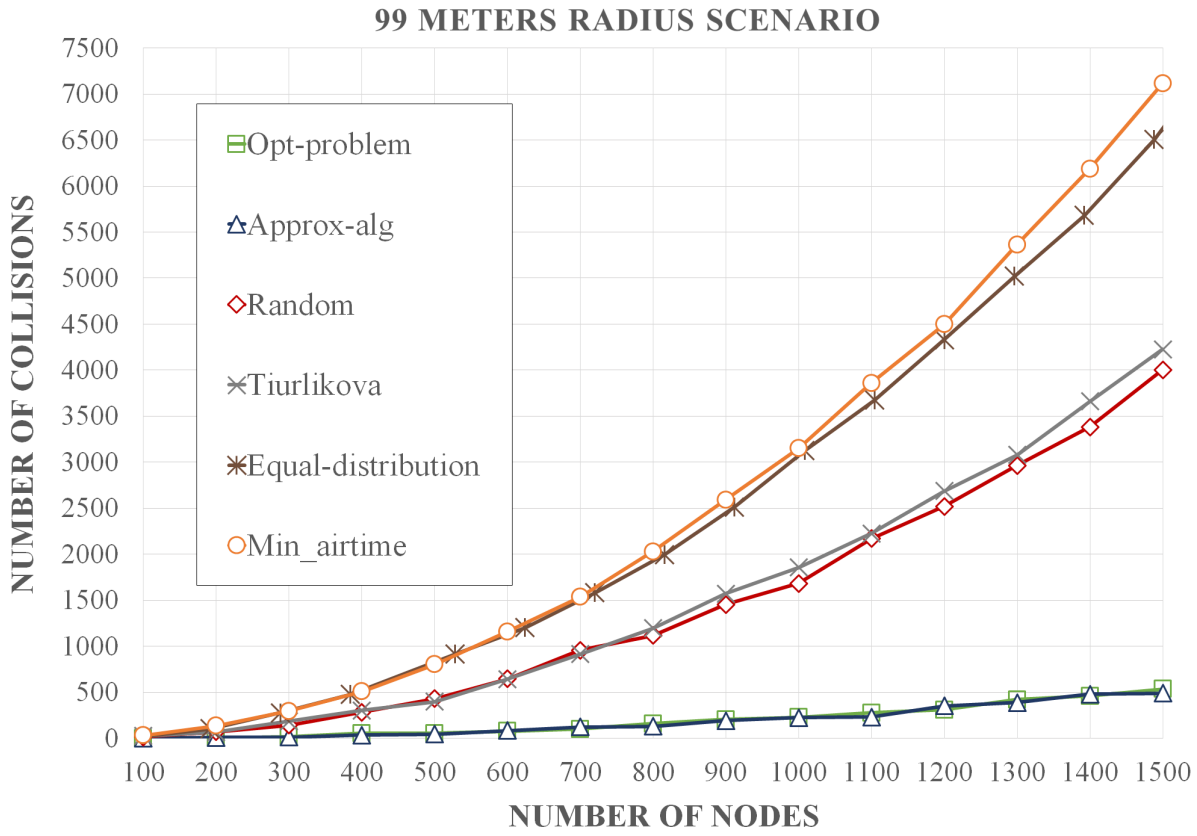

Source: Authorship.

The results in Figure 20 show that **opt-problem** and **approx-alg** cause the lowest *number of collisions*, being the curves represented in the graph practically equivalent. The policies **min-airtime**, **equal-distribution**, **Tiurlikova**, and **random** lead to average collision rates 13.3, 12.7, 7.8 and 7.4 times higher, respectively, in relation to **opt-problem** and **approx-alg**. Figure 21 demonstrates the *number of collisions* according to the number of nodes with gateway transmission range of 350 m.

Figure 21 – Number of collisions according to the number of nodes in the 350 m radius scenario.

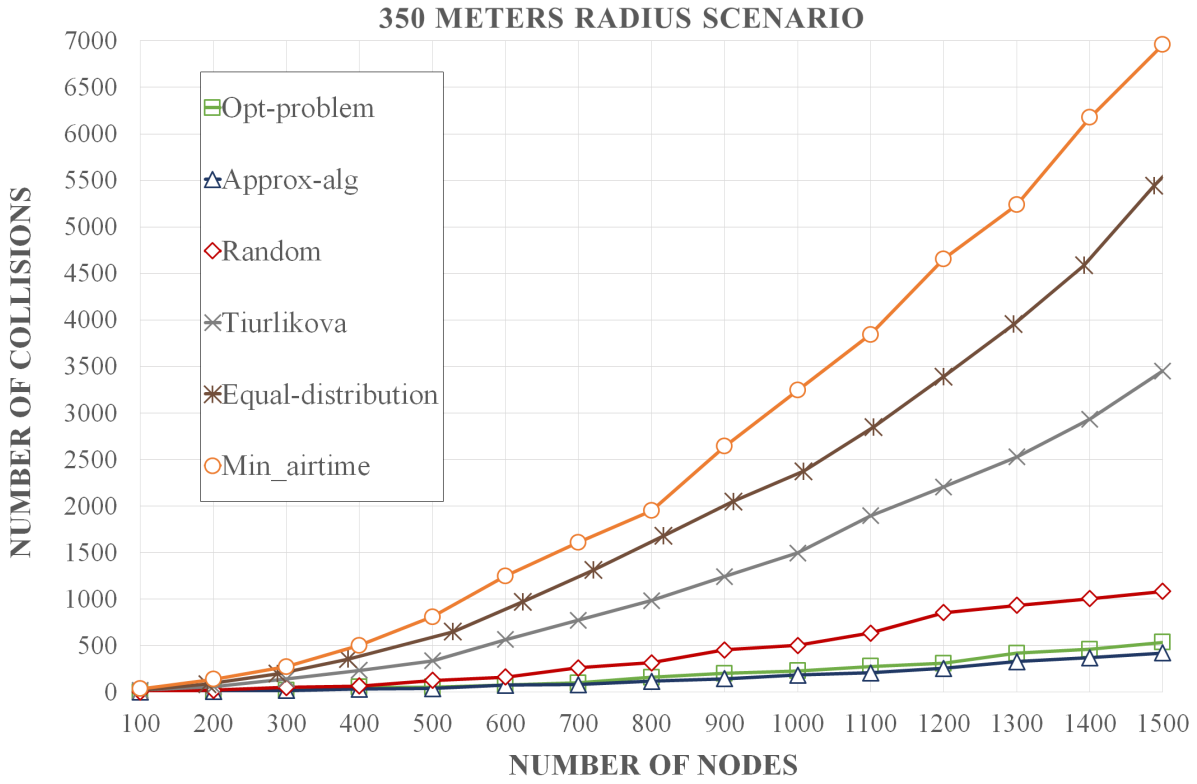

Source: Authorship.

The results in Figure 21 indicate that **opt-problem** and **approx-alg** have the smallest *number of collisions*, with equivalent results. The policies **min-airtime**, **equal-distribution**, **Tiurlikova**, and **random** have average collision rates 15.4, 11.7, 8.3 and 2.5 times higher, respectively, in relation to **opt-problem** and **approx-alg**.

The results shown for a radius of 99 m differ from 350 m in the number of collisions. The number of packet collisions for 350 m is about 12% higher, and this is reflected in the DER (as shown in Equation (20), DER is a function of the number collisions).

5.4 NETWORK ENERGY CONSUMPTION

The results for the 99 and 350 m scenarios are similar, because the calculation of *Network Energy Consumption*, as shown in Equation (22), depends on the number of packets sent, which is similar in the 99 and 350 m scenarios. Therefore, Figure 22 presents the *Network Energy Consumption* in mJ as a function of the number of nodes with a gateway transmission range of 99 m.

Figure 22 – Energy consumption as a function of the number of nodes in the 99 m radius scenario.

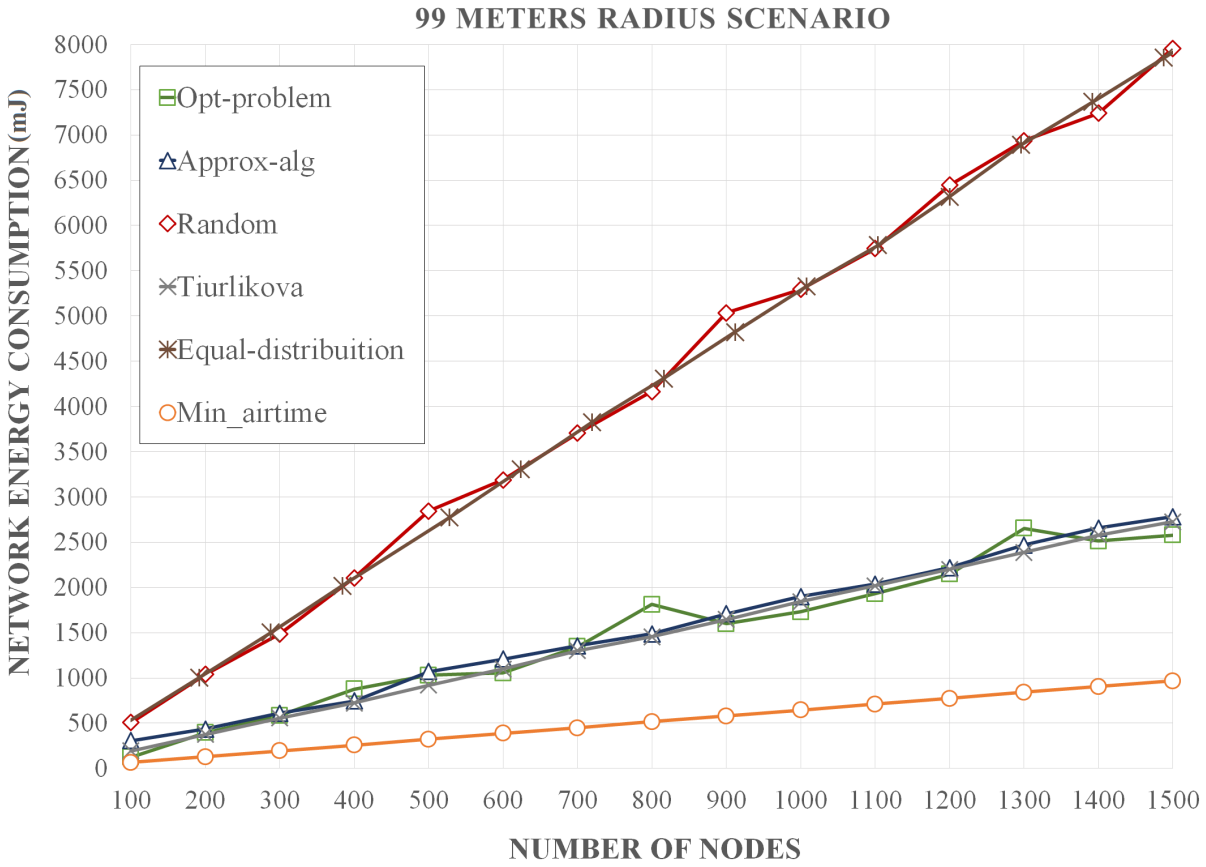

Source: Authorship.

The results in Figure 22 demonstrate that **equal-distribution** has a three times higher energy consumption rate as **opt-problem** and it is 2.94 greater than **approx-alg**. The **random** policy resulted in an average energy consumption 2.84 and 2.76 times higher than **opt-problem** and **approx-alg**, respectively. **Equal-distribution** and **random** achieved similar energy consumption, being 5.5% greater for **equal-distribution**. The difference in the average energy consumption between **opt-problem** and **approx-alg** is 2.7%. **Tiurlikova** achieved energy consumption similar to **opt-problem** and **approx-alg**. Both obtained an average consumption 2.9 times greater in relation to the **min-airtime**. Using this policy, SF is set to SF7, which has the lowest energy consumption, as reported in Section 2.1. However, in **opt-problem** and **approx-alg**, dynamic values of SF are assigned to the network nodes.

Figure 23 shows the *Network Energy Consumption* in mJ as a function of the number of nodes with a gateway transmission range of 350 m.

Figure 23 – Energy consumption as a function of the number of nodes - 350 m radius scenario.

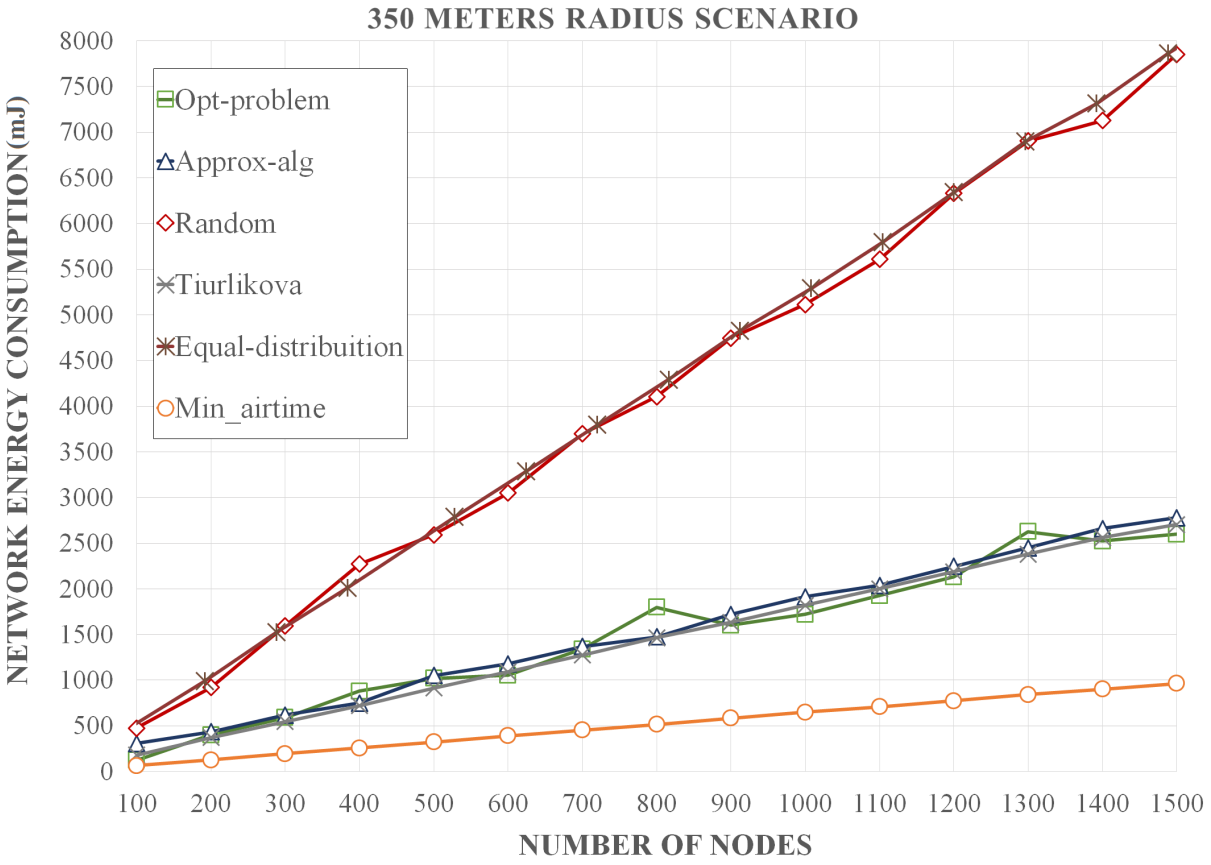

Source: Authorship.

The results in the Figure 23 demonstrates that **equal-distribution** has 8.65, 3.7, 3, 2.92 times more NEC than **min-airtime**, **Tiurlikova**, **opt-problem** and **approx-alg**, respectively. **equal-distribution** obtained a 7.6% higher NEC value than **random**. **approx-alg**, **opt-problem** and **Tiurlikova** obtained a NEC value of 2.96, 2.88 and 2.81 times higher than **min-airtime**. The dynamic policy with the best NEC value is the **Tiurlikova** policy, with an NEC 5.2% and 2.2% lower than the **approx-alg** and **opt-problem**, respectively.

The radio parameter assignment policies proposed in this work—**opt-problem** and **approx-alg**—proved to be better than policies **random**, **min-airtime**, **Tiurlikova**, and **equal-distribution** in relation to DER and *number of collisions*. The results show that **opt-problem** and **approx-alg** obtained DER values above 0.98 and 0.83 for the 99 m and 350 m scenarios, respectively. The *number of collisions* was minimal in relation to **random**, **min-airtime**, **Tiurlikova**, and **equal-distribution**. In addition, the energy consumption of the proposed optimization schemes is similar to **Tiurlikova** and lower when compared to other methods of dynamic assignment of values of SF and CF: **random** and **equal-distribution**.

5.5 ADR ANALYSIS AND COMPARISON IN APPROX-ALG AND RANDOM POLICIES

As explained in Section 4.2.2, the optimization of LoRaWAN network radio parameters proposed in this work is compatible with the standard LoRa protocol, which includes the ADR mechanism. In this context, we implemented the ADR mechanism in the *LoRaSim* simulator to analyze its impact on the **random** and **approx-alg** dynamic assignment policies, using, according to the DER, *number of collisions* and *Network Energy Consumption* evaluation metrics.

To represent a more overloaded network scenario, keeping the network simulation settings in Table 3, the average packet transmission period was changed from 16.6 min to 1 min with a transmission range of 99 m. Figures 24–26 illustrate the DER, the *number of collisions*, and the *Network Energy Consumption*, respectively, according to the number of nodes.

Figure 24 – DER as a function of the number of nodes in the 99 m radius scenario.

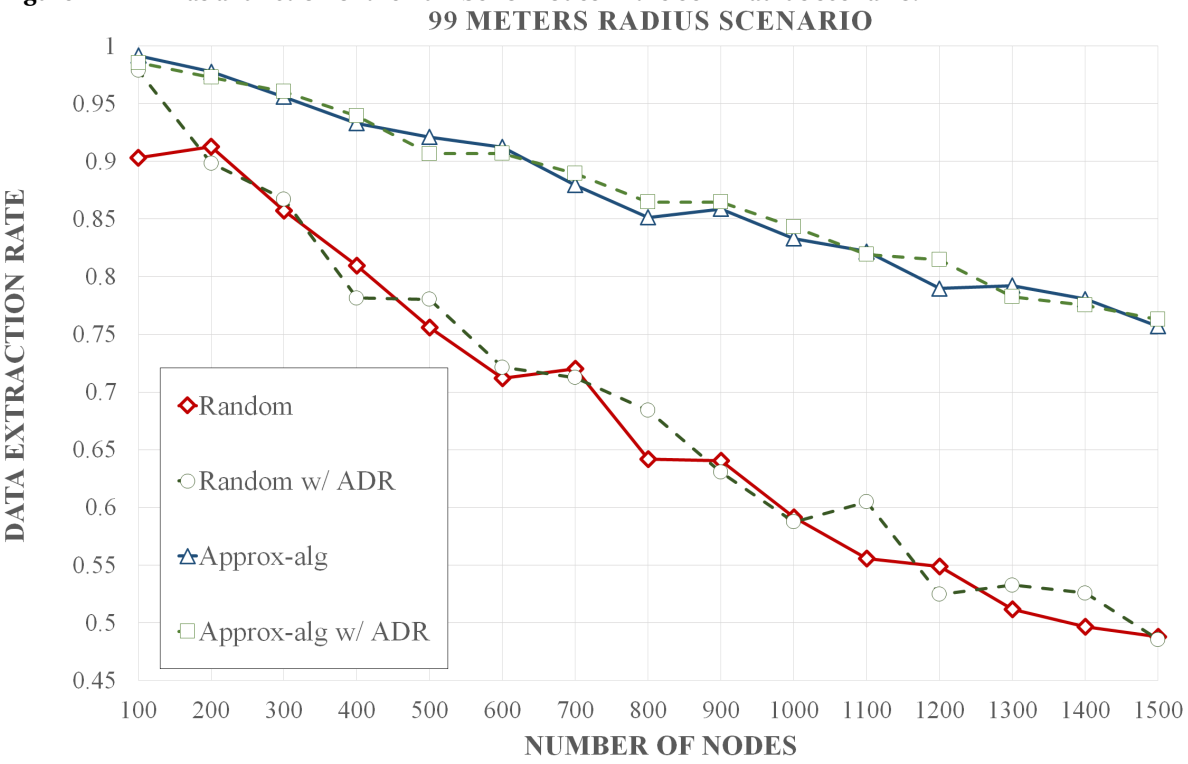

Source: Authorship.

According to Figure 24, the improvement of the **random** policy with the ADR mechanism is 1.43% compared to without ADR. The difference in **approx-alg** was smaller, only 0.23%. Therefore, it was the **random** policy that obtained the highest gain of DER with the ADR mechanism.

Figure 25 – Number of collisions according to the number of nodes in the 99 m radius scenario.

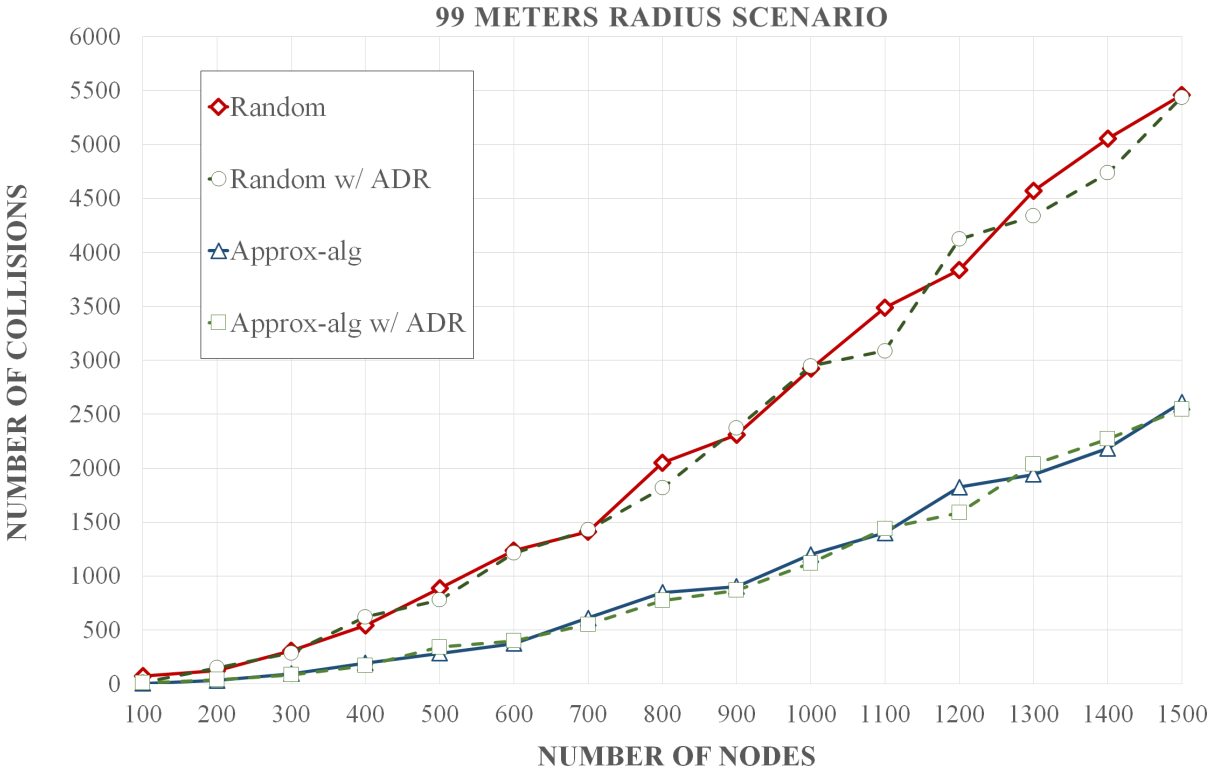

Source: Authorship.

Figure 25 shows that the network packet collision rate decreased around 2.79% in the **random** and 1.89% in the **approx-alg**.

Figure 26 – Energy consumption as a function of the number of nodes in the 99 m radius scenario.

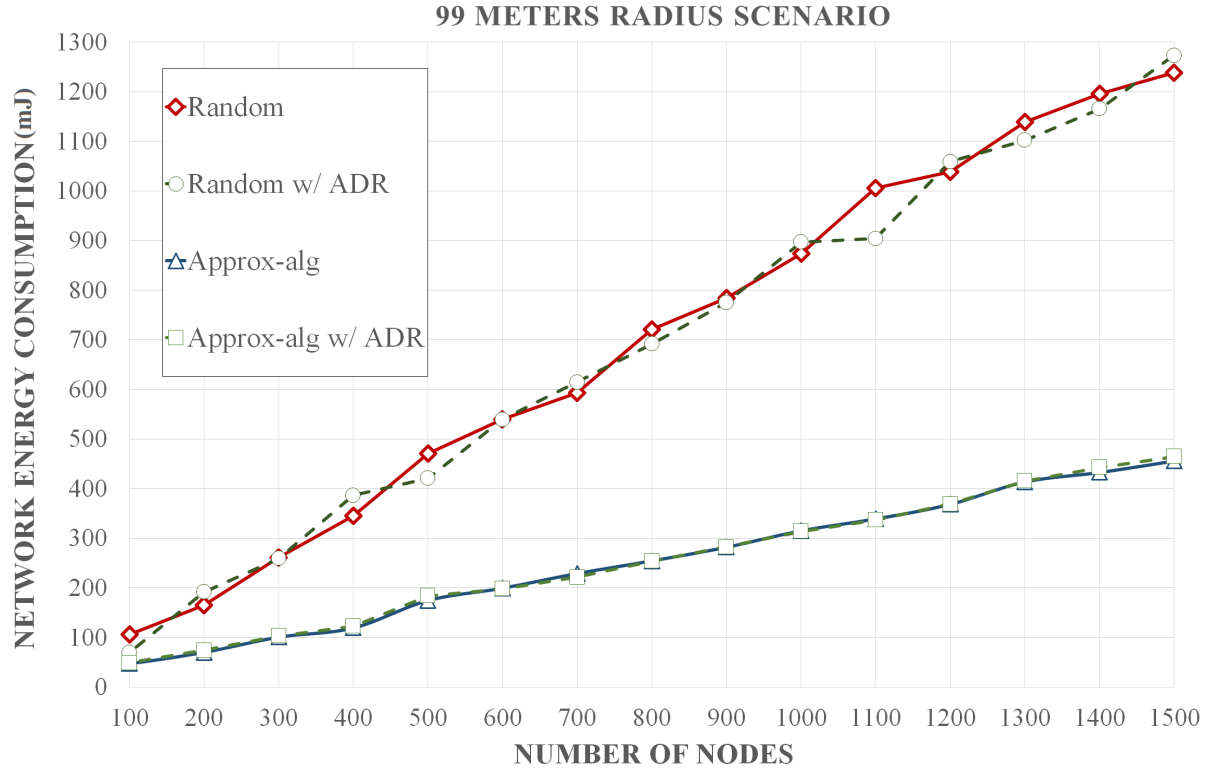

Source: Authorship.

Figure 26 shows that average NEC decreased 1.25% in the **random**. Therefore, the NEC value was very close in **approx-alg** with and without ADR. The results demonstrate that the **random** policy benefited from the ADR mechanism. However, the ADR mechanism difference in **approx-alg** is only noticeable in the collision rate.

5.6 THEORETICAL DATA RATE ANALYSIS

Applying Equation 4, the theoretical data rate in bps according to the number of nodes of the assignment policies is present in the graph of Fig. 27.

Figure 27 – Data rate according to the number of nodes

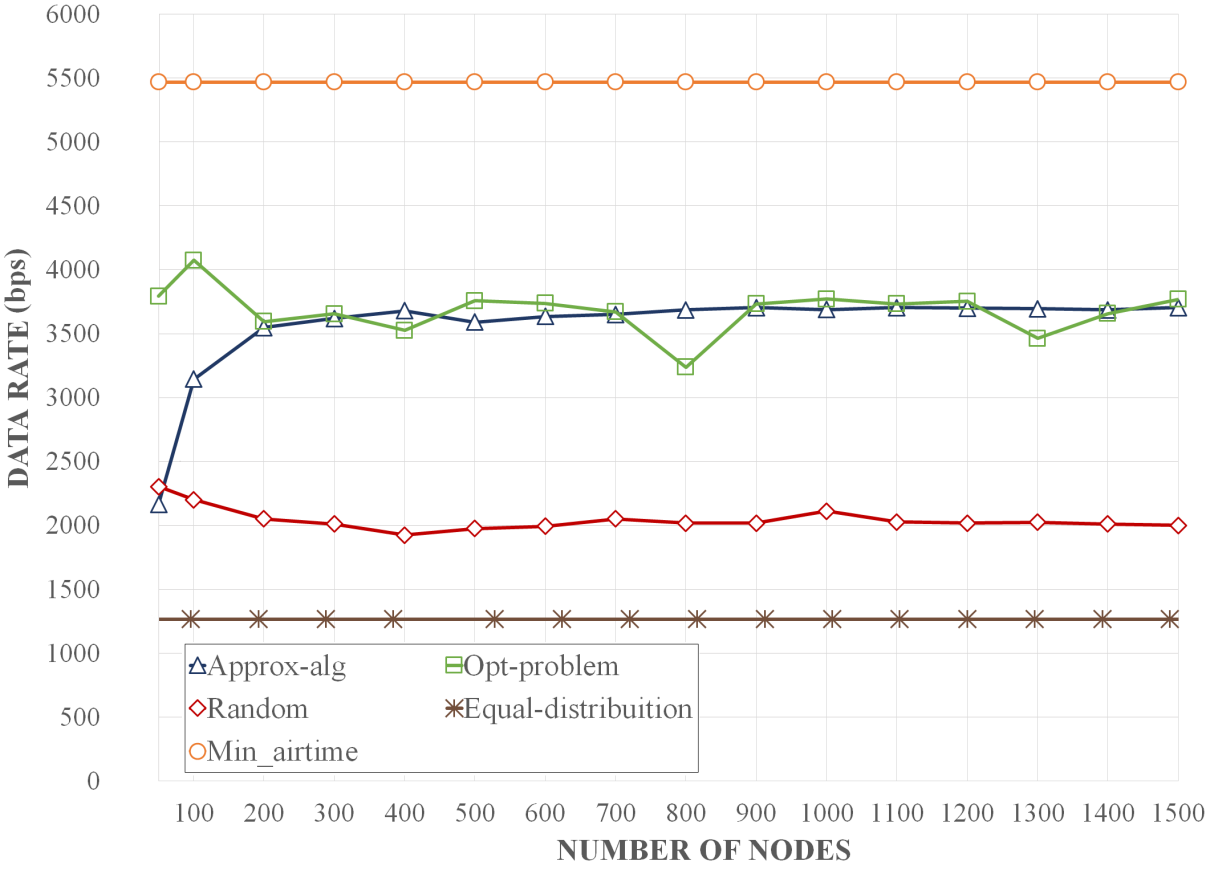

Source: Authorship.

According to the graph of Fig. 27 , the average data rate of the **opt-problem** and **approx-alg** assignment policies is 3683.29 bps and 3538.06 bps, respectively. The static **min-airtime** assignment policy obtained the highest average data rate of 5468.75 because the value of the SF parameter is fixed in SF7 for all nodes. Regarding the dynamic policies, the **opt-problem** obtained data rate of 2.9 and 1.75 times greater than **equal-distribution** and **random**, with a mean data rate of 1266.47 bps and 2046.18 bps, respectively.

5.7 ANALYSIS OF OVERHEADS INFERRED BY THE OPTIMIZATION PROPOSED IN THE STANDARD LORA PROTOCOL

The microcontroller in a LoRaWAN terminal processes sensor data and interfaces with the radio chip to transmit data over the network. The microcontroller must have enough memory for radio chip drivers, sensor drivers, and application code. Based on the recommended requirements for a microcontroller in a LoRaWAN terminal using the ® SX1267x radio chip, namely microcontroller 16 bit or 32 bit CPU, 16 KB RAM, and 256 KB flash memory (SEMTECH, 2017a), we analyze the possible overheads for end-device communication with the Approximation Algorithm application running on the LoRa Server caused by additional programming code:

(i) **Computation Time**: The Approximation Algorithm (Algorithm 3) has a linear complexity time O(n) = $111n + 57$, in the worst-case. Thus, since the Approximation Algorithm is expected to run in the LoRaWAN Application Layer and end-devices with a time complexity that is similar to the ADR mechanism (Algorithms 1 and 2), our optimization scheme causes no significant computation (time) overhead, neither in the end-devices nor in the LoRa Server. This is the best possible complexity in cases where the algorithm should sequentially read all of its input (CORMEN et al., 2009)

(ii) **Storage space**: The most significant part of the (optimization) algorithm runs in the LoRa Server, accounting for approximately 70 lines of code, while the extra code in the end-devices is around 60 lines. Overall, the implementation of our algorithm takes less than 20 kB of storage space (4 kB in average, 20 kB worst-case, considering different situations), which is not significant considering that most commercial off-the-shelf nodes have at least 128 kB of programming/non-volatile memory (minimum requirements for a LoRaWAN microcontroller (SEMTECH, 2017a));

(iii) **Energy consumption**: The proposed optimization scheme achieves lower *Network Energy Consumption* compared to other dynamic allocation policies. The way the Approximation Algorithm assigns end-devices pairs of (CF, SF), ordered from lowest to highest airtime, results in an improved network scalability (maximum number of nodes) ratio for lower power consumption. Regarding the **min-airtime** policy, which has shorter airtime due to using the SF parameter fixed in SF7, the simulation results show that the Approximation Algorithm consumed on average three times more energy.

(iv) **Communications**: Considering with Approximation Algorithm input an array of valid (SF, CF) pairs, end-devices only receive the (SF and CF) parameter values once (generated by the Approximation Algorithm). Our simulations show that the proposed optimization has a lower network packet send rate, as well as *number of collisions*, compared to the assignment policies **min-airtime**, **equal-distribution**, and **random**.

Therefore, the optimization proposal of this work causes no additional communication overhead.

6 CONCLUSION

We propose a simple yet efficient methodology to improve the performance of LoRaWAN networks by fine-tuning their SF and CF radio parameters, through *Mixed Integer Linear Programming* optimization approach. This enables the LoRaWAN network designer to choose the best network configuration. Importantly, these parameter assignment policies are backward compatible with the LoRa standard protocol, meaning that they can be implemented in commercial off-the-shelf LoRa devices.

Simulation results show that our methodology optimizes the assignment of CF and SF pairs with an average increase of 6.6% of DER about the standard LoRaWAN assignment, which assigns fixed CF and SF values between the End-devices so that the packets have the minimum air time. In comparison to networks where CF and SF pairs are dynamically assigned by the gateway, there is an increase of 5%, 2.9%, and 1.9% of DER to the Tiurlikova's, egalitarian and random distribution, respectively. Furthermore, our method leads to a *number of collisions* that is 13.3, 12.7, 7.8, and 7.4 times smaller than standard LoRaWAN, egalitarian, Tiurlikova's, and random distribution, respectively. In relation to the average energy consumption, the scenario with the standard LoRaWAN assignment, whose SF value set at 7, obtained an energy consumption 2.9 times lower than the proposed optimization. However, our optimization obtained a result similar to Tiurlikova's method, 3.92 and 2.73 times lower energy consumption than random distribution and egalitarian, respectively.

We are currently addressing the practical aspects of how to implement and integrate the proposed optimization mechanism in LoRa, guaranteeing backward compatibility with the standard protocol. Issues at stake are e.g. if/how this optimization can be made dynamically (run-time), with a predefined periodicity for all network nodes (in a synchronous way) or performed individually by each node.

REFERENCES

ABEELE, F. Van den et al. Scalability analysis of large-scale lorawan networks in ns-3. **IEEE Internet of Things Journal**, IEEE, v. 4, n. 6, p. 2186–2198, Dec 2017.

ABRAMSON, Norman M. The aloha system: another alternative for computer communications. In: **AFIPS Fall Joint Computing Conference**. [S.l.: s.n.], 1970.

ANATEL. **Portaria nº 50632, de 17 de dezembro de 2015**. 2015. <https://www.anatel.gov.br/legislacao/index.php/component/content/article?id=892>.

ANGRISANI, L. et al. Lora protocol performance assessment in critical noise conditions. In: **2017 IEEE 3rd International Forum on Research and Technologies for Society and Industry (RTSI)**. [S.l.: s.n.], 2017. p. 1–5.

BAIOCCHI, A.; RICCIATO, F. Analysis of pure and slotted aloha with multi-packet reception and variable packet size. **IEEE Communications Letters**, IEEE, p. 1–1, 2018. ISSN 1089-7798.

BANKOV, D.; KHOROV, E.; LYAKHOV, A. On the limits of lorawan channel access. In: **2016 International Conference on Engineering and Telecommunication (EnT)**. [S.l.: s.n.], 2016. p. 10–14.

BARRETO, André et al. 5g – wireless communications for 2020. **Journal of Communication and Information Systems**, v. 31, n. 1, Jun. 2016. Disponível em: <https://jcis.sbrt.org.br/jcis/article/view/384>.

BOR, Martin; ROEDIG, Utz. Lora transmission parameter selection. In: IEEE. **2017 13th International Conference on Distributed Computing in Sensor Systems (DCOSS)**. [S.l.], 2017. p. 27–34.

BOR, Martin C. et al. Do lora low-power wide-area networks scale? In: **Proceedings of the 19th ACM International Conference on Modeling, Analysis and Simulation of Wireless and Mobile Systems**. New York, NY, USA: ACM, 2016. (MSWiM '16), p. 59–67. ISBN 978-1-4503-4502-6. Disponível em: <http://doi.acm.org/10.1145/2988287.2989163>.

BORGHETTI, A. et al. An milp approach for short-term hydro scheduling and unit commitment with head-dependent reservoir. **IEEE Transactions on Power Systems**, IEEE, v. 23, n. 3, p. 1115–1124, Aug 2008. ISSN 0885-8950.

CASALS, Lluís et al. Modeling the energy performance of lorawan. **Sensors**, Multidisciplinary Digital Publishing Institute, v. 17, n. 10, p. 2364, 2017.

CATTANI, Marco; BOANO, Carlo; ROMER, Kay. An experimental evaluation of the reliability of lora long-range low-power wireless communication. **Journal of Sensor and Actuator Networks**, Multidisciplinary Digital Publishing Institute, v. 6, n. 2, p. 7, 2017.

CENTENARO, M. et al. Long-range communications in unlicensed bands: the rising stars in the iot and smart city scenarios. **IEEE Wireless Communications**, IEEE, v. 23, n. 5, p. 60–67, October 2016. ISSN 1536-1284.

COMMITTEE, LoRa Alliance Technical et al. Lorawan 1.1 specification. **LoRa Alliance Stand**, v. 1, n. 1, 2017.

CORMEN, Thomas H et al. **Introduction to algorithms**. [S.l.]: MIT press, 2009.

EARL, M. G.; D'ANDREA, R. Iterative milp methods for vehicle-control problems. **IEEE Transactions on Robotics**, IEEE, v. 21, n. 6, p. 1158–1167, Dec 2005. ISSN 1552-3098.

EGLI, Peter R. **LPWAN Low Power Wide Area Network: Overview of emerging technologies for low power wide area networks in internet of things and m2m scenarios**. 2015. <http://indigoo.com/dox/itdp/12_MobileWireless/LPWAN.pdf>.

FELTRIN, L. et al. Lorawan: Evaluation of link- and system-level performance. **IEEE Internet of Things Journal**, IEEE, v. 5, n. 3, p. 2249–2258, June 2018.

GLOBAL MARKET INSIGHTS. **Global LPWAN Market Size worth over $65 Bn by 2025**. 2019. <https://www.gminsights.com/pressrelease/lpwan-market>.

____. **Semtech and Helium Expand LoRaWAN Network Deployments**. 2020. <https://iotbusinessnews.com/2020/08/27/06404-semtech-and-helium-expand-lorawan-network-deployments/>.

GOUNARIS, Chrysanthos E et al. Designing networks: A mixed-integer linear optimization approach. **Networks**, Wiley Online Library, v. 68, n. 4, p. 283–301, 2016.

IBM. **CPLEX Optimizer**. 2019. <https://www.ibm.com/analytics/cplex-optimizer>.

IOT ANALYTICS. **5 things to know about the LPWAN market in 2020**. 2020. <https://iot-analytics.com/5-things-to-know-about-the-lpwan-market-in-2020/>.

KHUTSOANE, Oratile; ISONG, Bassey; ABU-MAHFOUZ, Adnan M. Iot devices and applications based on lora/lorawan. In: IEEE. **IECON 2017-43rd Annual Conference of the IEEE Industrial Electronics Society**. [S.l.], 2017. p. 6107–6112.

KLEINROCK, L.; TOBAGI, F. Packet switching in radio channels: Part i - carrier sense multiple-access modes and their throughput-delay characteristics. **IEEE Transactions on Communications**, IEEE, v. 23, n. 12, p. 1400–1416, December 1975. ISSN 0090-6778.

LEE, Gyeongheon; YOUN, Joosang. Group-based transmission scheduling scheme for building lora-based massive iot. In: IEEE. **2020 International Conference on Artificial Intelligence in Information and Communication (ICAIIC)**. [S.l.], 2020. p. 583–586.

LIM, J. T.; HAN, Y. Spreading factor allocation for massive connectivity in lora systems. **IEEE Communications Letters**, IEEE, v. 22, n. 4, p. 800–803, April 2018. ISSN 1089-7798.

LIMA, Ricardo M; GROSSMANN, Ignacio E. Computational advances in solving mixed integer linear programming problems. **Chemical Engineering Greetings to Prof. Sauro Pierucci, AIDAC**, v. 151, p. 160, 2011.

LORA ALLIANCE. **LoRa Server**. [S.l.]: GitHub, 2019. <https://github.com/brocaar/loraserver>.

LORA SERVER. **The LoRa Server project**. <https://www.loraserver.io/overview/>.

MÉNDEZ, CA; HENNING, GP; CERDÁ, J. An milp continuous-time approach to short-term scheduling of resource-constrained multistage flowshop batch facilities. **Computers & Chemical Engineering**, Elsevier, v. 25, n. 4-6, p. 701–711, 2001.

MIKHAYLOV, K.; PETAEJAEJAERVI, Juha; HAENNINEN, T. Analysis of capacity and scalability of the lora low power wide area network technology. In: **European Wireless 2016; 22th European Wireless Conference**. [S.l.: s.n.], 2016. p. 1–6.

NAVARRO-ORTIZ, J. et al. Integration of lorawan and 4g/5g for the industrial internet of things. **IEEE Communications Magazine**, IEEE, v. 56, n. 2, p. 60–67, Feb 2018. ISSN 0163-6804.

NEUMANN, P.; MONTAVONT, J.; NOëL, T. Indoor deployment of low-power wide area networks (lpwan): A lorawan case study. In: **2016 IEEE 12th International Conference on Wireless and Mobile Computing, Networking and Communications (WiMob)**. [S.l.: s.n.], 2016. p. 1–8.

NOREEN, U.; BOUNCEUR, A.; CLAVIER, L. A study of lora low power and wide area network technology. In: **2017 International Conference on Advanced Technologies for Signal and Image Processing (ATSIP)**. [S.l.: s.n.], 2017. p. 1–6.

PETÄJÄJÄRVI, Juha et al. Performance of a low-power wide-area network based on lora technology: Doppler robustness, scalability, and coverage. **International Journal of Distributed Sensor Networks**, SAGE Publications Sage UK: London, England, v. 13, n. 3, p. 1550147717699412, 2017.

PETAJAJARVI, J. et al. On the coverage of lpwans: range evaluation and channel attenuation model for lora technology. In: **2015 14th International Conference on ITS Telecommunications (ITST)**. [S.l.: s.n.], 2015. p. 55–59.

RAZA, U.; KULKARNI, P.; SOORIYABANDARA, M. Low power wide area networks: An overview. **IEEE Communications Surveys Tutorials**, IEEE, v. 19, n. 2, p. 855–873, Secondquarter 2017.

REYNDERS, B. et al. Improving reliability and scalability of lorawans through lightweight scheduling. **IEEE Internet of Things Journal**, IEEE, v. 5, n. 3, p. 1830–1842, June 2018.

RICHARDS, A.; HOW, J. P. Aircraft trajectory planning with collision avoidance using mixed integer linear programming. In: **Proceedings of the 2002 American Control Conference (IEEE Cat. No.CH37301)**. [S.l.: s.n.], 2002. v. 3, p. 1936–1941 vol.3. ISSN 0743-1619.

SALLUM, Eduardo et al. **LoRa_CF_SF_assignment_optimization**. [S.l.]: GitHub, 2019. <https://github.com/esallum/LoRa_CF_SF_assignment_optimization>.

____. Improving quality-of-service in lora low-power wide-area networks through optimized radio resource management. **Journal of Sensor and Actuator Networks**, Multidisciplinary Digital Publishing Institute, v. 9, n. 1, p. 10, 2020.

____. Performance optimization on lora networks through assigning radio parameters. In: IEEE. **2020 IEEE International Conference on Industrial Technology (ICIT)**. [S.l.], 2020. p. 304–309.

SAMSATLI, Sheila; SAMSATLI, Nouri J. A multi-objective milp model for the design and operation of future integrated multi-vector energy networks capturing detailed spatio-temporal dependencies. **Applied Energy**, Elsevier, v. 220, p. 893–920, 2018.

SARKAR, Nurul I. The impact of transmission overheads on ieee 802.11 throughput: analysis and simulation. Cyber Journal, 2011.

SEMTECH. **LoRaWAN – simple rate adaptation recommended algorithm**. 2016. <https://www.thethingsnetwork.org/forum/uploads/default/original/2X/7/7480e044aa93a54a910dab8ef0adfb5f515d14a1.pdf>. Acesso em: 10 de maio de 2019.

____. **MCU Requirements for LoRaWAN**. 2017. <https://www.semtech.com/uploads/documents/AN1200.28_MCU_Requirements_for_LoRaWAN_V3.pdf>. Acesso em: 10 de maio de 2019.

____. **SX1301 Datasheet**. 2017. <https://www.semtech.com/uploads/documents/sx1301.pdf>. Acesso em: 18 de setembro de 2019.

____. **SX1272/3/6/7/8: LoRa Modem**. 2019. <https://www.semtech.com/uploads/documents/LoraDesignGuide_STD.pdf>. Acesso em: 10 de maio de 2019.

SIGFOX. **Sigfox, the world's leading IoT services provider.** 2019. <https://www.sigfox.com/en>. Acesso em: 25 de março de 2019.

SLABICKI, Mariusz; PREMSANKAR, Gopika; FRANCESCO, Mario Di. Adaptive configuration of lora networks for dense iot deployments. In: IEEE. **NOMS 2018-2018 IEEE/IFIP Network Operations and Management Symposium**. [S.l.], 2018. p. 1–9.

TERRA. **IoT: Net Sensors lança bueiros inteligentes e antidengue com tecnologia LoRa de baixo custo**. 2020. <https://www.terra.com.br/noticias/dino/iot-net-sensors-lanca-bueiros-inteligentes-e-antidengue-com-tecnologia-lora-de-baixo-custo,84cab4eb67b2c5e6baa022abb2232fc03ioqt41t.html>.

THE THINGS INDUSTRIES. **API Reference**. 2019. <https://www.thethingsnetwork.org/docs/applications/mqtt/api.html#uplink-messages>. Acesso em: 17 de junho de 2019.

____. **Building a global open LoRaWAN network**. 2019. <https://www.thethingsnetwork.org/>. Acesso em: 25 de março de 2019.

____. **Duty Cycle for LoRaWAN Devices**. 2019. <https://www.thethingsnetwork.org/docs/lorawan/duty-cycle.html>. Acesso em: 10 de setembro de 2019.

____. **LoRaWAN Adaptive Data Rate**. 2019. <https://www.thethingsnetwork.org/docs/applications/mqtt/api.html#uplink-messages>. Acesso em: 17 de junho de 2019.

Tiurlikova, A.; Stepanov, N.; Mikhaylov, K. Method of assigning spreading factor to improve the scalability of the lorawan wide area network. In: **2018 10th International Congress on Ultra Modern Telecommunications and Control Systems and Workshops (ICUMT)**. [S.l.: s.n.], 2018. p. 1–4.

TOUSSAINT, J.; RACHKIDY, N. El; GUITTON, A. Performance analysis of the on-the-air activation in lorawan. In: **2016 IEEE 7th Annual Information Technology, Electronics and Mobile Communication Conference (IEMCON)**. [S.l.: s.n.], 2016. p. 1–7.

UFOP. **Pesquisadores desenvolvem oxímetro para monitoramento de pacientes com Covid-19 a distância**. 2020. <https://ufop.br/noticias/coronavirus/pesquisadores-desenvolvem-oximetro-para-monitoramento-de-pacientes-com-covid-19>.

VANGELISTA, L. Frequency shift chirp modulation: The lora modulation. **IEEE Signal Processing Letters**, IEEE, v. 24, n. 12, p. 1818–1821, Dec 2017. ISSN 1070-9908.

VATCHARATIANSAKUL, N.; TUWANUT, P.; PORNAVALAI, C. Experimental performance evaluation of lorawan: A case study in bangkok. In: **2017 14th International Joint Conference on Computer Science and Software Engineering (JCSSE)**. [S.l.: s.n.], 2017. p. 1–4.

VOIGT, Thiemo et al. Mitigating inter-network interference in lora networks. In: **Proceedings of the 2017 International Conference on Embedded Wireless Systems and Networks**. USA: Junction Publishing, 2017. (EWSN ’17), p. 323–328. ISBN 978-0-9949886-1-4. Disponível em: <http://dl.acm.org/citation.cfm?id=3108009.3108093>.

WAVIOT. **WAVIoT LPWAN – Low-power long-range (LPWAN) solutions for IoT and M2M**. 2019. <https://waviot.com/>. Acesso em: 25 de março de 2019.

WEIGHTLESS SIG. **What is Weightless - Weightless**. 2019. <http://www.weightless.org/about/what-is-weightless>. Acesso em: 25 de março de 2019.

WI-FI ALLIANCE. **Wi-Fi HaLow**. 2019. <https://www.wi-fi.org/discover-wi-fi/wi-fi-halow>. Acesso em: 25 de março de 2019.

XIONG, X. et al. Low power wide area machine-to-machine networks: key techniques and prototype. **IEEE Communications Magazine**, IEEE, v. 53, n. 9, p. 64–71, September 2015. ISSN 0163-6804.

YOUSUF, A. M.; ROCHESTER, E. M.; GHADERI, M. A low-cost lorawan testbed for iot: Implementation and measurements. In: **2018 IEEE 4th World Forum on Internet of Things (WF-IoT)**. [S.l.: s.n.], 2018. p. 361–366.

ZHENG, W. et al. Synthesis of task and message activation models in real-time distributed automotive systems. In: **2007 Design, Automation Test in Europe Conference Exhibition**. [S.l.: s.n.], 2007. p. 1–6. ISSN 1530-1591.

ZHU, Q. et al. Optimizing the software architecture for extensibility in hard real-time distributed systems. **IEEE Transactions on Industrial Informatics**, IEEE, v. 6, n. 4, p. 621–636, Nov 2010. ISSN 1551-3203.

ZORBAS, Dimitrios; O'FLYNN, Brendan. Autonomous collision-free scheduling for lora-based industrial internet of things. In: IEEE. **2019 IEEE 20th International Symposium on"A World of Wireless, Mobile and Multimedia Networks"(WoWMoM)**. [S.l.], 2019. p. 1–5.